Distributed stochastic reserve scheduling in AC power systems with uncertain generation

Rostampour, Vahab; Ter Haar, Ole; Keviczky, Tamas

Important note
To cite this publication, please use the final published version (if applicable).
Please check the document version above.

Distributed Stochastic Reserve Scheduling in AC Power Systems With Uncertain Generation

Vahab Rostampour ⓘ, Ole ter Haar, and Tamás Keviczky ⓘ

Abstract—**This paper presents a framework to carry out multi-area stochastic reserve scheduling (RS) based on an ac optimal power flow (OPF) model with high penetration of wind power using distributed consensus and the alternating direction method of multipliers (ADMM). We first formulate the OPF-RS problem using semidefinite programming (SDP) in infinite-dimensional spaces that is in general computationally intractable. Using a novel affine policy, we develop an approximation of the infinite-dimensional SDP as a tractable finite dimensional SDP, and explicitly quantify the performance of the approximation. To this end, we adopt the recent developments in randomized optimization that allow *a priori* probabilistic feasibility guarantees to optimally schedule power generating units while simultaneously determining the geographical allocation of the required reserve. We then use the geographical pattern of the power system to decompose the large-scale system into a multi-area power network, and provide a consensus ADMM algorithm to find a feasible solution for both local and overall multi-area network. Using our distributed stochastic framework, each area can use its own wind information to achieve local feasibility certificates, while ensuring overall feasibility of the multi-area power network under mild conditions. We provide numerical comparisons with a new benchmark formulation, the so-called converted dc (CDC) power flow model, using Monte Carlo simulations for two different IEEE case studies.**

Index Terms—**AC power systems, distributed stochastic consensus ADMM, distributed scenario program, distributed stochastic reserve allocations, multi-area AC power systems, stochastic reserve scheduling.**

I. INTRODUCTION

POWER transmission system operators (TSOs) aim to find an economic operating point to satisfy the power demand and network constraints by solving an optimal power flow (OPF) problem. TSOs have to deal with increasing degrees of uncertainty due to high penetration of wind power generation. While wind power has clear environmental advantages, it is a highly variable and not fully controllable resource. This imposes novel challenges and tasks for TSOs to avoid blackouts, outages, etc.,

and highlights the necessity of introducing a new paradigm to existing TSO functionalities.

The reserve scheduling (RS) task of TSOs deals with day-ahead scheduling of the reserve power to accommodate possible mismatches between forecasted and actual wind power. Stochastic variants of the RS problem, where violations are allowed with a small probability to achieve better performance, have received a lot of attention in the past few years, see [1]–[4] and the references therein. A stochastic RS problem is typically formulated using a lossless DC model based on the assumption of constant voltage magnitudes and small voltage angles, while ignoring the active power losses [5]. It is worth mentioning that these assumptions do not hold in general and may lead to sub-optimality or even infeasibility when implemented on real-world systems, especially for networks under a high degree of stress [6]. Using an AC representation of the power network enables the stochastic RS formulation to accurately model the effect of large deviations of wind power from its forecasted value, and to offer a-priori suitable reserves such that both active and reactive power, and complex-valued voltage are globally optimal. However, due to the non-convexity of the OPF problem, identifying such an optimal operating point of a power system may not be straightforward. In [7], different reformulations and relaxations of the AC OPF problem were presented and their connections were discussed. By means of semidefinite programming (SDP), in [7] a convex relaxation was provided under the existence of a rank-one SDP solution to guarantee the recovery of a globally optimal solution of the power network.

The RS problem incorporating an OPF formulation has been introduced in [8], where a chance-constrained OPF problem was formulated. With some modifications, motivated by practical aspects of the problem, the authors in [8] provided a theoretical guarantee that the OPF-RS problem yields a rank-one feasible solution. Using a heuristic Monte Carlo sampling approach, they showed that the resulting optimization problem involves an OPF problem for each wind power profile. Our work in this paper is motivated by [8] to first rigorously provide theoretical guarantees for the feasibility of physical constraints, and then, develop a distributed reserve scheduling framework for the AC model of power network, which is, to best of our knowledge, has not been addressed in the related works. Even though the authors in [8] presented a complete day-ahead OPF-RS formulation with up- and down spinning reserves, the results in the aforementioned references are limited either to be heuristic or to a single hourly-based RS with the relaxed conditions. The major barrier for representing OPF-RS prob-

lems as a SDP is the necessity of defining a square SDP matrix variable, which makes the cardinality of scalar variables of the OPF-RS problem quadratic with respect to the number of buses in the power network. This may yield a very large-scale SDP problem for realistic large-scale power networks of interest.

Dealing with a chance-constrained AC OPF problem has recently received a lot of attention in literature, see e.g., [9]–[14]. Our work in this paper differs from the aforesaid references in two important aspects. We first formulate the AC OPF problem by considering the uncertain wind power generations. Using a similar convexification to [7], we incorporate the stochastic RS into the convexified AC OPF formulation. This results in a large-scale SDP in infinite-dimensional spaces. We then provide a systematical approach to move from infinite to semi-infinite and then to finite-dimensional spaces using a novel affine policy. Such a policy differs from the existing one in the literature, see, e.g., [4], [8], [13], [14] and references therein, in technical and practical aspects, and significantly reduces the worst-case computational complexity (WCCC). Theoretical results for the level of the approximation and a priori feasibility certificates are provided by adopting the recent developments in randomized optimization that do not require any prior knowledge of uncertainty bounds or distributions. The proposed policy enjoys the property of operational rule of the so-called automatic generation regulator (AGR) concept in power systems. Affine policies have been also used for the OPF problem using DC model of power system, e.g., [15], and most recently, in [16] for the AGR actions (up- and downspinning reserves).

We next introduce a decomposition technique by leveraging the geographical pattern in power systems to decompose the high-dimensional SDP into small-scale SDPs related to each area of a multi-area power network. We employ recent results in graph theory to break down the large-scale positive-semidefinite (PSD) constraints into small-sized constraints. Such a technique has been also considered in [17] for state estimation problem in power systems. We then provide a distributed consensus framework using the alternating direction method of multipliers (ADMM), similarly to [18]–[21], with some modifications for the AC OPF problem in power system. We extend such a distributed framework to handle the stochastic RS problem using the AC OPF model of a multi-area network which has not, to the best of our knowledge, been considered in literature. We highlight that such an extension is possible using the proposed affine policy which overcomes the difficulty of having defined a square SDP matrix variable for all possible wind trajectories, see, e.g., [4], [8], [13], [14], [22]. We also note that in our proposed distributed stochastic framework, each area of the power system can have its own measurements of wind power, while having feasibility guarantees for both local and overall multi-area power network under mild conditions. Two different simulation results using IEEE benchmark case studies are provided to illustrate the functionality of our developments. We also provide a new benchmark formulation for stochastic RS using DC model of power system, namely converted DC (CDC) to demonstrate more realistic comparisons. The main contributions of this paper are twofold:

1) We provide a novel reformulation of the RS problem using an AC OPF model of power systems with wind power

generations, leading to an infinite-dimensional SDP which is in general computationally intractable. We propose an approximation of the infinite-dimensional SDP with tractable finite-dimensional SDPs using an affine policy inspired by practical aspects of the problem. While finalizing the review process of this paper, a similar affine policy was simultaneously proposed in [16] using DC OPF to solve the problem with a similar structure, i.e., the uncertainty set is unknown and unbounded. We then explicitly quantify the exactness of the approximation and provide a priori probabilistic feasibility guarantees to optimally schedule generating units while simultaneously determining the geographical allocation of the required reserve. We also provide another formulation of the OPF-RS problem, similar to [8] with some modifications, and compare these in terms of WCCC analysis.

2) We develop a distributed stochastic framework to carry out multi-area RS using an AC OPF model of power networks with wind power generations. We provide a technique to decompose a large-scale finite dimensional SDP into small-scale problems by exploring the connections between the properties of a power network and chordal graphs. A noticeable feature of our distributed setup is that each local area of the power system may have different local accuracy regarding available wind power and receives a priori probabilistic feasibility certificates to optimally schedule local generating units together with local allocation of the required reserve. This is based on the recent results in [23]. We then provide consensus ADMM algorithms for both OPF and OPF-RS problems in a similar manner to [20], [21] with some modifications to cope with stochasticity of the formulations.

II. PROBLEM FORMULATION

A. AC OPF Problem

Consider a power system with a set of buses $\mathcal{N}$, a set of lines $\mathcal{L} \subseteq \mathcal{N} \times \mathcal{N}$ and a set of generator buses $\mathcal{G} \subseteq \mathcal{N}$ such that $|\mathcal{N}| = N_b$ and $|\mathcal{G}| = N_G$. The set of wind power generation buses is denoted by $\mathcal{F} \subseteq \mathcal{N}$ such that $|\mathcal{F}| = N_w$, and $\mathcal{G} \bigcap \mathcal{F} = \emptyset$ which means there is no wind power at generator buses[1]. The set $\mathcal{T}$ forms a day-ahead hourly-based horizon of the RS optimization problem and in this paper $|\mathcal{T}| = 24$. The vectors $\boldsymbol{p} \in \mathbb{R}^{N_b}, \boldsymbol{q} \in \mathbb{R}^{N_b}$ and $\boldsymbol{s} \in \mathbb{C}^{N_b}$ denote real, reactive and apparent power, respectively. Superscripts G, D, w are also used to indicate generated, demanded and wind power, respectively.

Define the decision variables to be the generator dispatch $\boldsymbol{p}_t^G, \boldsymbol{q}_t^G \in \mathbb{R}^{N_G}$ and the complex bus voltages $\boldsymbol{v}_t \in \mathbb{C}^{N_b}$ for each time step $t \in \mathcal{T}$. For the sake of brevity, a tilde denotes a set of variables over all time steps, e.g., $\tilde{\boldsymbol{a}} := \{\boldsymbol{a}_t\}_{t \in \mathcal{T}}$. Using the rectangular voltage notation: $\boldsymbol{x}_t := [\mathrm{Re}\,(\boldsymbol{v}_t)^\top \, \mathrm{Im}\,(\boldsymbol{v}_t)^\top]^\top \in \mathbb{R}^{2N_b}$, we follow [7, Lemma 1] to determine the data-matrices $Y_k, Y_k^*, Y_{lm}, Y_{lm}^*, M_k$. The cost function is the cost of real power generation, expressed as a second-order polynomial [24], see

---

[1]This is considered to streamline the presentation and it is not restrictive for our proposed framework.

(1a) below, where the coefficient vectors $\boldsymbol{c}^{\mathrm{qu}}, \boldsymbol{c}^{\mathrm{li}} \in \mathbb{R}_+^{N_G}$ correspond to the quadratic and linear cost coefficients, respectively, and $[\boldsymbol{c}^{\mathrm{qu}}]$ represents a diagonal matrix with entries $\boldsymbol{c}^{\mathrm{qu}}$. We now formulate the AC OPF problem by taking into account the effect of wind power generation as follows:

$$\underset{\tilde{\boldsymbol{x}}, \tilde{\boldsymbol{p}}^G, \tilde{\boldsymbol{q}}^G}{\text{minimize}} \quad \sum_{t \in \mathcal{T}} (\boldsymbol{c}^{\mathrm{li}})^\top \boldsymbol{p}_t^G + (\boldsymbol{p}_t^G)^\top [\boldsymbol{c}^{\mathrm{qu}}] \boldsymbol{p}_t^G \quad (1a)$$

subject to:

1) Power generation limits $\forall k \in \mathcal{G}, \forall t \in \mathcal{T}$:

$$\underline{p_k^G} \le p_{k,t}^G \le \overline{p_k^G},$$
$$\underline{q_k^G} \le q_{k,t}^G \le \overline{q_k^G}. \quad (1b)$$

2) Power balance at every bus $\forall k \in \mathcal{N}, \forall t \in \mathcal{T}$:

$$\boldsymbol{x}_t^\top Y_k \boldsymbol{x}_t = p_{k,t}^G - p_{k,t}^D + p_{k,t}^w,$$
$$\boldsymbol{x}_t^\top Y_k^* \boldsymbol{x}_t = q_{k,t}^G - q_{k,t}^D, \quad (1c)$$

where $\boldsymbol{p}_t^w := \{p_{k,t}^w\}_{k \in \mathcal{F}}$ is the wind power, and $\boldsymbol{s}_t^D := \{s_{k,t}^D\}_{k \in \mathcal{N}}$ is the demanded power such that $s_{k,t}^D = p_{k,t}^D + q_{k,t}^D$.

3) Bus voltage limits $\forall k \in \mathcal{N}, \forall t \in \mathcal{T}$:

$$|\underline{v_k}|^2 \le \boldsymbol{x}_t^\top M_k \boldsymbol{x}_t \le |\overline{v_k}|^2. \quad (1d)$$

4) Lineflow limits $\forall (l, m) \in \mathcal{L}, \forall t \in \mathcal{T}$:

$$\left(\boldsymbol{x}_t^\top Y_{lm} \boldsymbol{x}_t \right)^2 + \left(\boldsymbol{x}_t^\top Y_{lm}^* \boldsymbol{x}_t \right)^2 \le |\overline{s_{lm}}|^2,$$

which can be reformulated using the Schur-complement [25] to form a linear matrix inequality constraint, such that the fourth-order dependence on the voltage vector is reduced to quadratic terms:

$$\begin{bmatrix} -|\overline{s_{lm}}|^2 & \boldsymbol{x}_t^\top Y_{lm} \boldsymbol{x}_t & \boldsymbol{x}_t^\top Y_{lm}^* \boldsymbol{x}_t \\ \boldsymbol{x}_t^\top Y_{lm} \boldsymbol{x}_t & -1 & 0 \\ \boldsymbol{x}_t^\top Y_{lm}^* \boldsymbol{x}_t & 0 & -1 \end{bmatrix} \preceq 0. \quad (1e)$$

5) Reference bus constraint $\forall t \in \mathcal{T}$:

$$\boldsymbol{x}_t^\top E_{\mathrm{ref}} \boldsymbol{x}_t = 0, \quad (1f)$$

where $E_{\mathrm{ref}} \in \mathbb{R}^{2N_b \times 2N_b}$ is a diagonal matrix from the standard basis vector $e_{N_b + i_{\mathrm{ref}}} \in \mathbb{R}^{2N_b}$, and i_{ref} denotes the reference bus.

Remark 1: The power balance constraints (1c) can be used to reformulate the real and reactive generator dispatch in terms of the voltage vector as follows $\forall k \in \mathcal{N}, \forall t \in \mathcal{T}$:

$$p_{k,t}^G = \boldsymbol{x}_t^\top Y_k \boldsymbol{x}_t + p_{k,t}^D - p_{k,t}^w, \quad (2a)$$
$$q_{k,t}^G = \boldsymbol{x}_t^\top Y_k^* \boldsymbol{x}_t + q_{k,t}^D. \quad (2b)$$

Using this reformulation, one can substitute for $p_{k,t}^G$ and $q_{k,t}^G$ in (1b) to have $\forall k \in \mathcal{N}, \forall t \in \mathcal{T}$:

$$\underline{p_k^G} \le \boldsymbol{x}_t^\top Y_k \boldsymbol{x}_t + p_{k,t}^D - p_{k,t}^w \le \overline{p_k^G}, \quad (3a)$$
$$\underline{q_k^G} \le \boldsymbol{x}_t^\top Y_k^* \boldsymbol{x}_t + q_{k,t}^D \le \overline{q_k^G}, \quad (3b)$$

where the lower and upper generation limits have been also extended to $\mathcal{N}$ using $\underline{p_k^G} = \overline{p_k^G} = 0 \, \forall k \in \{\mathcal{N} \setminus \mathcal{G}\}$.

Remark 2: Following Remark 1, one can reformulate the cost function (1a) using the voltage vector $\boldsymbol{x}_t$:

$$f_G^x(\boldsymbol{x}_t, \boldsymbol{p}_t^w, \boldsymbol{p}_t^D) := \sum_{k \in \mathcal{G}} c_k^{\mathrm{li}} \left(\boldsymbol{x}_t^\top Y_k \boldsymbol{x}_t + p_{k,t}^D - p_{k,t}^w \right)$$
$$+ c_k^{\mathrm{qu}} \left(\left(\boldsymbol{x}_t^\top Y_k \boldsymbol{x}_t + p_{k,t}^D - p_{k,t}^w \right) \right)^2. \quad (4)$$

It is important to note that this function is of order four with respect to $\boldsymbol{x}_t$, but it can be also made quadratic.[2] To streamline the presentation, these steps are skipped.

Using $\tilde{\boldsymbol{x}}$, we reformulate the problem (1) in a more compact form:

$$\text{OPF}(\tilde{\boldsymbol{p}}^w) : \begin{cases} \underset{\tilde{\boldsymbol{x}}}{\text{minimize}} & \sum_{t \in \mathcal{T}} f_G^x(\boldsymbol{x}_t, \boldsymbol{p}_t^w, \boldsymbol{p}_t^D) \\ \text{subject to} & (1d), (1e), (1f), (3) \end{cases}.$$

$\text{OPF}(\tilde{\boldsymbol{p}}^w)$ is a quadratically constrained quadratic program (QCQP) in $\tilde{\boldsymbol{x}}$, and a non-convex optimization problem, since the data matrices $Y_k, Y_k^*, Y_{lm}, Y_{lm}^*$ are indefinite [7], which is in fact an NP-hard problem [26] and hard to solve.

It is important to mention that the physical constraints such as generator on/off, min up and min down time limits, ramping limits, are not taken into consideration. Integrating such constraints is the topic of our ongoing research, which aims at developing a unified framework to solve the so-called unit commitment (UC) together with RS problem using AC OPF model of the power system.

B. Convexified AC OPF Problem

We can reformulate $\text{OPF}(\tilde{\boldsymbol{p}}^w)$ as an equivalent problem in a matrix variable $W_t := \boldsymbol{x}_t \boldsymbol{x}_t^\top \in \mathbb{S}^{2N_b}$ using a semi-definite reformulation (SDR) technique, see, e.g., [7], [27] and the references therein. W_t represents the operating state of the network at time step t, and therefore, it is called the state matrix. We define $\mathcal{W} \subset \mathbb{S}^{2N_b}$ as the set of feasible operating states constraints, such that $W_t \in \mathcal{W}$, using the following characteristics:

$$\mathcal{W}(\boldsymbol{p}^w, \boldsymbol{s}^D) := \Big\{ W \in \mathbb{S}^{2N_b} \,\Big|\, \mathrm{Tr}\,(E_{\mathrm{ref}} W) = 0$$

$$\underline{p_k^G} \le \mathrm{Tr}\,(Y_k W) + p_k^D - p_k^w \le \overline{p_k^G}, \quad \forall k \in \mathcal{N},$$

$$\underline{q_k^G} \le \mathrm{Tr}\,(Y_k^* W) + q_k^D \le \overline{q_k^G}, \quad \forall k \in \mathcal{N},$$

$$|\underline{v_k}|^2 \le \mathrm{Tr}\,(M_k W) \le |\overline{v_k}|^2, \forall k \in \mathcal{N}, \forall (l, m) \in \mathcal{L},$$

$$\begin{bmatrix} -|\overline{s_{lm}}|^2 & \mathrm{Tr}\,(Y_{lm} W) & \mathrm{Tr}\,(Y_{lm}^* W) \\ \mathrm{Tr}\,(Y_{lm} W) & -1 & 0 \\ \mathrm{Tr}\,(Y_{lm}^* W) & 0 & -1 \end{bmatrix} \preceq 0 \Big\}.$$

$$(5)$$

---

[2]The cost function can be made linear with the use of the epigraph notation (see also [25, Section 4.1.3]). The resulting inequality constraint can be converted to a LMI using the Schur complement (see also [25, Section A.5.5]), which yields a quadratic function of x.

Consider now the following formulation as an equivalent optimization problem to OPF($\tilde{\boldsymbol{p}}^w$):

$$\underset{\tilde{W}}{\text{minimize}} \quad \sum_{t \in \mathcal{T}} f_G(W_t, \boldsymbol{p}_t^w, \boldsymbol{p}_t^D) \tag{6a}$$

$$\text{subject to} \quad W_t \in \mathcal{W}(\boldsymbol{p}_t^w, \boldsymbol{s}_t^D), \qquad \forall t \in \mathcal{T}, \tag{6b}$$

$$W_t \succeq 0, \qquad \forall t \in \mathcal{T}, \tag{6c}$$

$$\text{rank}(W_t) = 1, \qquad \forall t \in \mathcal{T}, \tag{6d}$$

where f_G is defined by (4) and $W_t = \boldsymbol{x}_t \boldsymbol{x}_t^\top$. Constraints (6c) and (6d) are introduced to guarantee the exactness of SDR, and consequently, OPF($\tilde{\boldsymbol{p}}^w$) and (6) are equivalent.

The optimization problem (6) is non-convex, due to the presence of rank-one constraint (6d). Removing (6d) relaxes the problem to an SDP. It has been shown in [7] and later in [28] that the rank-one constraint can be dropped without affecting the solution for most power networks. In particular, in [7, Lemma 2] the authors presented that if the relaxed problem (the SDP problem without rank-one constraint) has a rank-one solution, then it must have an infinite number of rank-two solutions. Later, in [8, Proposition 1], the authors showed that when the convex relaxation of the AC OPF problem has solutions with rank at most two, then, forcing any arbitrary selected entry of the diagonal of the matrix W_t to be zero results in a rank-one optimal solution. This condition is practically motivated since the voltage angle of one of the buses (the reference bus) is often fixed at zero in practice. We denote by C-OPF($\tilde{\boldsymbol{p}}^w$) the convexified version of OPF($\tilde{\boldsymbol{p}}^w$) problem in $\tilde{W}$, i.e., Problem (6) with the rank-one constraint (6d) removed.

In the following proposition, we restate the results in [8, Proposition 1] to highlight that our developments, in the following parts, build on these results and therefore the obtained solution for the state variables using our proposed approach is the rank-one feasible solution.

Proposition 1: If the C-OPF($\tilde{\boldsymbol{p}}^w$) problem has solutions with rank at most two, then, forcing any arbitrary selected entry of the diagonal of matrix W_t to be zero results in a rank-one solution W_t^*. Moreover, the corresponding value of the objective function of the proposed optimization is identical to that of the original OPF($\tilde{\boldsymbol{p}}^w$) problem.

It is important to note that guaranteeing the optimality of the obtained solutions using the proposed approach is not included in the scope of this paper and it is subject of our ongoing research work. Instead, in this paper we focus on the topic of feasibility and deriving probabilistic guarantees for constraint fulfillment in a distributed setting.

C. Convexified AC OPF Reserve Scheduling Problem

Consider a power network where a TSO aims to solve a day-ahead AC OPF problem to determine an optimal generator dispatch for the forecasted wind power trajectory such that: 1) the equipment in the power system remains safe and 2) the power balance in the power network is achieved. As a novel feature in our proposed formulation C-OPF($\tilde{\boldsymbol{p}}^w$) has a dependency on $\tilde{\boldsymbol{p}}^w$, and thus, it solves the AC OPF problem while taking into account the actual wind power trajectory $\tilde{\boldsymbol{p}}^w$. We here define

the difference between a generic actual wind power realization and the forecasted wind power as the mismatch wind power at each time step, e.g. $\boldsymbol{p}_t^m = \boldsymbol{p}_t^w - \boldsymbol{p}_t^{w,f}$. Due to the fact that $\tilde{\boldsymbol{p}}^m := \{\boldsymbol{p}_t^m\}_{t \in \mathcal{T}}$ is a random variable, the following technical assumption is necessary in order to proceed to the next steps.

Assumption 1: $\tilde{\boldsymbol{p}}^m$ is defined on some probability space $(\mathcal{P}, \mathfrak{B}(\mathcal{P}), \mathbb{P})$, where $\mathfrak{B}(\cdot)$ denotes a Borel σ-algebra, and $\mathbb{P}$ is a probability measure defined over $\mathcal{P}$.

As a top priority of TSOs is to ensure the feasibility and validity of the power network, we formulate the following problem:

$$\underset{\tilde{W}^f, \tilde{W}}{\text{minimize}} \quad \sum_{t \in \mathcal{T}} f_G(W_t^f, \boldsymbol{p}_t^{w,f}, \boldsymbol{p}_t^D) \tag{7a}$$

$$\text{subject to} \quad W_t^f \in \mathcal{W}(\boldsymbol{p}_t^{w,f}, \boldsymbol{s}_t^D), \qquad \forall t \in \mathcal{T}, \tag{7b}$$

$$W_t \in \mathcal{W}(\boldsymbol{p}_t^w, \boldsymbol{s}_t^D), \forall \tilde{\boldsymbol{p}}^m \in \mathcal{P}, \quad \forall t \in \mathcal{T}, \tag{7c}$$

$$W_t^f \succeq 0, W_t \succeq 0 \qquad \forall t \in \mathcal{T}, \tag{7d}$$

where $\tilde{\boldsymbol{p}}_t^m = \tilde{\boldsymbol{p}}^w - \tilde{\boldsymbol{p}}^{w,f}$ and $\tilde{\boldsymbol{p}}^{w,f}$ denotes the forecasted wind power trajectory, $\tilde{\boldsymbol{p}}^w$ is a generic wind power trajectory, $\tilde{W}^f$ is related to the state of the network in the case of forecasted wind power, and $\tilde{W}$ is a generic network state for a generic wind power trajectory. Constraints (7b) and (7c) ensure feasibility for every network state, while constraints (7d) enforce PSDness of the forecasted network state and the generic network state for all possible wind power trajectories.

As a second task of the TSO, the power balance of the power network has to be achieved to ensure demand satisfaction even in the presence of uncertain wind power generation. To address this issue, the TSO employs *reserve power scheduling*, using the fact that a mismatch between actual wind power and forecasted wind power can be mitigated by the controllable generators [1]. We can thus express $r_{k,t} := p_{k,t}^G - p_{k,t}^{G,f}$ where $\boldsymbol{r}_t = \{r_{k,t}\}_{k \in \mathcal{G}} \in \mathbb{R}^{N_G}$ denotes the amount of reserve requirement in the power network. By Substituting $p_{k,t}^G = \text{Tr}(Y_k W_t) + p_{k,t}^D - p_{k,t}^w$ and $p_{k,t}^{G,f} = \text{Tr}\left(Y_k W_t^f\right) + p_{k,t}^D - p_{k,t}^{w,f}$, one can obtain the reserve power in terms of the network states W_t and W_t^f as follows:

$$r_{k,t} = \text{Tr}\left(Y_k\left(W_t - W_t^f\right)\right). \tag{8}$$

The elements of $\boldsymbol{r}_t = \{r_{k,t}\}_{k \in \mathcal{N}_G}$ can be positive and negative to represent the up- and downspinning reserve powers, respectively, such that they are deployed for a power deficit and surplus to bring balance to the network and satisfy the demand [24]. We thus distinguish between up- and downspinning reserve powers using $\boldsymbol{r}_t^{ds}, \boldsymbol{r}_t^{us} \in \mathbb{R}^{N_G}$ such that $\forall t \in \mathcal{T}$:

$$-\boldsymbol{r}_t^{ds} \leq \boldsymbol{r}_t \leq \boldsymbol{r}_t^{us}, \ 0 \leq \boldsymbol{r}_t^{us}, \ 0 \leq \boldsymbol{r}_t^{ds}, \tag{9}$$

where r_t^{us} and r_t^{ds} are enforced to be positive as they only appear in the reserve cost function. We now consider corresponding linear up- and downspinning cost coefficients $\boldsymbol{c}^{us}, \boldsymbol{c}^{ds} \in \mathbb{R}_+^{N_G}$ yielding the total reserve cost:

$$f_R(\boldsymbol{r}_t^{us}, \boldsymbol{r}_t^{ds}) := (c^{us})^\top \boldsymbol{r}_t^{us} + (c^{ds})^\top \boldsymbol{r}_t^{ds}.$$

The mismatches between the demanded power and uncertain generation (wind) induce frequency deviations and activate the

primary and secondary frequency controller (Automatic Generation Regulation (AGR)). The existence of an ideal primary frequency control functionality compensating for any fast time scale power deviation is assumed. Here, we focus only on the steady state behavior of the AGR reserve mechanism [4] and define two vectors $\boldsymbol{d}_t^{\text{us}}, \boldsymbol{d}_t^{\text{ds}} \in \mathbb{R}^{N_G}$ to distribute the amount of up- or downspinning reserve powers among the available generators for each hour $t \in \mathcal{T}$. To obtain the optimal control strategies for AGR, we consider the following equality constraint, $\forall \boldsymbol{p}_t^m \in \mathcal{P}$, $\forall k \in \mathcal{G}$ and $\forall t \in \mathcal{T}$:

$$\text{Tr}\left(Y_k(W_t - W_t^f)\right) = -d_{k,t}^{\text{us}} \min(\boldsymbol{p}_t^m, 0) - d_{k,t}^{\text{ds}} \max(\boldsymbol{p}_t^m, 0). \tag{10}$$

In order to always negate the wind power mismatch using the reserve power and bring balance to the power network, we enforce the sum of the distribution vectors to be equal to one using the following constraint $\forall t \in \mathcal{T}$:

$$\sum_{k \in \mathcal{G}} d_{k,t}^{\text{us}} = 1 \,, \quad \sum_{k \in \mathcal{G}} d_{k,t}^{\text{ds}} = 1 \,. \tag{11}$$

Using $\Xi := \left\{\tilde{W}^f, \tilde{W}, \tilde{\boldsymbol{d}}^{\text{us}}, \tilde{\boldsymbol{d}}^{\text{ds}}, \tilde{\boldsymbol{r}}^{\text{us}}, \tilde{\boldsymbol{r}}^{\text{ds}}\right\}$ as the set of decision variables, and combining our previous discussions with the optimization problem (7), we are now in the position to formulate C-OPF($\tilde{\boldsymbol{p}}^w$) with RS problem as follows:

$$\text{C-OPF-RS}: \begin{cases} \min_{\Xi} & \sum_{t \in \mathcal{T}} \left(f_G(W_t^f, \boldsymbol{p}_t^{w,f}) + f_R(\boldsymbol{r}_t^{\text{us}}, \boldsymbol{r}_t^{\text{ds}})\right) \\ \text{s.t.} & (7b), (7c), (7d), (10), (11), (9) \end{cases}.$$

C-OPF-RS is an uncertain infinite dimensional SDP in the sense that the dimension of the decision spaces as well as the number of constraints are both infinite, due to the unknown and unbounded set $\mathcal{P}$. It is therefore computationally intractable and in general difficult to solve. In the following section, we develop an approximation technique to provide a tractable finite dimensional SDP optimization problem.

III. PROPOSED TRACTABLE REFORMULATION

In this section, we propose two different reformulations for C-OPF-RS problem, and study conditions under which one can provide a finite approximation. We approach this goal in two different ways. We first develop a novel affine policy to translate the problem into semi-infinite dimensional spaces, and then provide a finite approximation to the semi-infinite SDP using randomization technique. As a second approach, we directly employ a randomized technique to provide a finite approximation for the C-OPF-RS problem. The solution of each of these methods comes with a priori probabilistic performance certificates. We finally provide the WCCC analysis for both proposed methods.

A. Infinite to Semi-Infinite Program: Affine Policy

Consider the proposed equality constraint (10). Since the uncertain set $\mathcal{P}$ is unknown and unbounded, it is straightforward to see that the dimension of the decision spaces for the variable W_t as well as the number of constraints are both infinite.

To overcome this difficulty, we propose an *affine policy* to restrict the decision space using a *conic combination* of the generic network state W_t in C-OPF-RS. Observe that in (10), the network state variable W_t for every realization of the uncertainty in each time step, can be represented as a linear combination of the network forecasted state W_t^f and the up- and downspinning reserve distributions. This is also practically inspired by the AGR mechanism.

Motivated by this observation, we propose a novel parametrization of the generic network state that encodes this restriction implicitly. Define $\hat{W}_t(\boldsymbol{p}_t^m) \in \mathbb{S}^{2N_b}$ to be the parametrized generic network state $\tilde{\boldsymbol{p}}^m \in \mathcal{P}, \forall t \in \mathcal{T}$ in the following form:

$$\hat{W}_t(\boldsymbol{p}_t^m) := W_t^f + W_t^{\text{us}} \max(-\boldsymbol{p}_t^m, 0) + W_t^{\text{ds}} \max(\boldsymbol{p}_t^m, 0), \tag{12}$$

where $W_t^{\text{us}}, W_t^{\text{ds}} \in \mathbb{S}^{2N_b}$ are the coefficient matrix variables for every $t \in \mathcal{T}$. The parametrization of the network state as a conic combination of PSD matrices is, to the best of our knowledge, a novel way to make this type of problems more manageable. While preparing the final version of this work, [16] independently proposed a similar affine policy, a so-called surrogate affine approximation, for DC OPF problem with unknown and unbounded uncertainty set together with an interesting comparison with the conventional affine policy.

Using the proposed conic parametrization, the generic network state is decomposed into a deterministic component and two components that scale with the positive or negative uncertainty. It is worth mentioning that both $\max(\boldsymbol{p}_t^m, 0)$ and $\max(-\boldsymbol{p}_t^m, 0)$ are always non-negative and never simultaneously non-zero such that the change in network state is determined by either W_t^{ds} or W_t^{us} in case of either a wind power surplus or deficit, respectively. The following theorem can be considered as the main result of this section to approximate C-OPF-RS in semi-infinite dimensional spaces.

Theorem 1: Given the proposed affine policy in (12), an exact approximation of the C-OPF-RS problem can be formulated using the following optimization problem by defining $\hat{\Xi} := \left\{\tilde{W}^f, \tilde{W}^{\text{us}}, \tilde{W}^{\text{ds}}, \tilde{\boldsymbol{r}}^{\text{us}}, \tilde{\boldsymbol{r}}^{\text{ds}}\right\}$ as the new set of decision variables:

$$\text{P-OPF-RS}: \begin{cases} \min_{\hat{\Xi}} & \sum_{t \in \mathcal{T}} \left(f_G(W_t^f, \boldsymbol{p}_t^{w,f}) + f_R(\boldsymbol{r}_t^{\text{us}}, \boldsymbol{r}_t^{\text{ds}})\right) \\ \text{s.t.} & W_t^f \in \mathcal{W}(\boldsymbol{p}_t^{w,f}, \boldsymbol{s}_t^D) \\ & \hat{W}_t(\boldsymbol{p}_t^m) \in \mathcal{W}(\boldsymbol{p}_t^{w,f} + \boldsymbol{p}_t^m, \boldsymbol{s}_t^D) \\ & W_t^f \succeq 0, \quad W_t^{\text{us}} \succeq 0, \quad W_t^{\text{ds}} \succeq 0 \\ & -\boldsymbol{r}_t^{\text{ds}} \leq \boldsymbol{r}_t \leq \boldsymbol{r}_t^{\text{us}}, 0 \leq \boldsymbol{r}_t^{\text{us}}, 0 \leq \boldsymbol{r}_t^{\text{ds}} \\ & \sum_{k \in \mathcal{G}} \text{Tr}\left(Y_k W_t^{\text{us}}\right) = 1 \\ & \sum_{k \in \mathcal{G}} \text{Tr}\left(Y_k W_t^{\text{ds}}\right) = -1 \\ & \forall \tilde{\boldsymbol{p}}^m \in \mathcal{P}, \forall t \in \mathcal{T} \end{cases},$$

where $\boldsymbol{r}_t = \{r_{k,t}\}_{k \in \mathcal{G}}$ should be replaced with

$$r_{k,t} = -\text{Tr}\left(Y_k W_t^{\text{us}}\right) \min(\boldsymbol{p}_t^m, 0) + \text{Tr}\left(Y_k W_t^{\text{ds}}\right) \max(\boldsymbol{p}_t^m, 0).$$

Proof: The proof is provided in the Appendix. ∎

The interpretation of Theorem 1 is as follows. Due to the fact that the formulation in C-OPF-RS follows a linear decision rule concept as a consequence of the AGR mechanism, C-OPF-RS and P-OPF-RS are equivalent formulations using the proposed affine policy (12).

Remark 3: The distribution vectors of reserve power, $\tilde{\boldsymbol{d}}^{\text{us}}, \tilde{\boldsymbol{d}}^{\text{ds}}$ are encoded in $\tilde{W}^{\text{us}}, \tilde{W}^{\text{ds}}$, respectively, through the equality constraints[3], and therefore, these can be determined a-posteriori using the following relations $\forall k \in \mathcal{G}, \forall t \in \mathcal{T}$:

$$d_{k,t}^{\text{us}} = \text{Tr}\left(Y_k W_t^{\text{us}}\right) \ , \ d_{k,t}^{\text{ds}} = -\text{Tr}\left(Y_k W_t^{\text{ds}}\right) \ .$$

One can also define $\tilde{\boldsymbol{d}}^{\text{us}}, \tilde{\boldsymbol{d}}^{\text{ds}}$ as two additional decision vector and replace the two equality constraints in P-OPF-RS with the following constraints:

$$d_{k,t}^{\text{us}} = \text{Tr}\left(Y_k W_t^{\text{us}}\right) \ , \ d_{k,t}^{\text{ds}} = \text{Tr}\left(Y_k W_t^{\text{ds}}\right), \tag{13}$$

$$\sum_{k\in\mathcal{G}} d_{k,t}^{\text{us}} = 1 \ , \ \sum_{k\in\mathcal{G}} d_{k,t}^{\text{ds}} = -1 \ . \tag{14}$$

The P-OPF-RS problem is a semi-infinite dimensional SDP due to the uncountable number of constraints corresponding to the uncertainty set $\mathcal{P}$, which is indeed an unbounded and unknown uncertainty set. In the following section, we adopt a randomization technique to approximate the P-OPF-RS problem and obtain a finite-dimensional SDP. We will also provide a performance guarantee for the feasibility of constraints in a probabilistic sense with a high level of confidence.

B. Semi-Infinite to Finite Program: Randomized Approach

We develop a finite approximation to the semi-infinite SDP in P-OPF-RS problem that is in general hard to solve and known to be computationally intractable [30]. To overcome this difficulty, we employ the recent developments in the area of randomized optimization, leading to a priori probabilistic guarantees for the feasibility of the obtained solutions.

Recall the randomization technique by assuming to have a 'sufficient number' of independent and identically distributed (i.i.d.) samples of the string of wind power mismatch realizations $\tilde{\boldsymbol{p}}^m = \{\boldsymbol{p}_t^m\}_{t\in\mathcal{T}}$, which can be obtained either empirically or by a random scenario generator. Notice that $\boldsymbol{p}_t^m$ at each sampling time t is not necessarily i.i.d., and in particular, it may have time-varying distributions and/or be correlated in time. We denote $\mathcal{S} := \{\tilde{\boldsymbol{p}}^{m,1}, \ldots, \tilde{\boldsymbol{p}}^{m,N_s}\} \in \mathcal{P}^{N_s}$ as a set of given finite multi-extraction samples (scenarios) from $\mathcal{P}$. Consider now a tractable version of P-OPF-RS using the following finite-dimensional

SDP optimization problem:

$$\text{SP-OPF-RS} : \begin{cases} \underset{\hat{\Xi}\in\hat{\mathcal{X}}}{\text{minimize}} & f(\hat{\Xi}) \\ \text{subject to} & \hat{g}(\hat{\Xi}, \tilde{\boldsymbol{p}}^{m,i}) \leq 0 \ , \ \forall \tilde{\boldsymbol{p}}^{m,i} \in \mathcal{S} \end{cases},$$

where $\hat{g}(\cdot)$ is the uncertain constraint function of P-OPF-RS, and all other constraints for P-OPF-RS are used to construct $\hat{\mathcal{X}}$, a deterministic feasible set for the P-OPF-RS problem.

The key features of the proposed tractable optimization problem (SP-OPF-RS) are as follows:

- there is no need to know the probability measure $\mathbb{P}$ explicitly, only the capability of obtaining random scenarios is enough.
- formal results to quantify the robustness of the obtained approximations are available. In particular the results follow the so-called scenario approach [31], which allow to bound a-priori the violation probability of the obtained solution via SP-OPF-RS.

In the following theorem, we restate the explicit theoretical bound of [31, Theorem 1] which measures the finite scenario behavior of SCP.

Theorem 2: Let $\varepsilon \in (0, 1)$, $\beta \in (0, 1)$ and $N_s \geq \mathsf{N}(\varepsilon, \beta, d)$, such that

$$\mathsf{N}(\varepsilon, \beta, d) := \min\left\{ N \in \mathbb{N} \ \Big| \ \sum_{i=0}^{d-1} \binom{N}{i} \varepsilon^i (1-\varepsilon)^{N-i} \leq \beta \right\} \ .$$

where d is the number of decision variables in P-OPF-RS problem. If the optimizer $(\hat{\Xi}^*)$ of SP-OPF-RS is applied to P-OPF-RS, then the original uncertain constraint function $\hat{g}(\cdot)$ in P-OPF-RS is satisfied with probability $1 - \varepsilon$ and with confidence level higher than $1 - \beta$.

It was shown in [31] that the above bound is tight. The interpretation of Theorem 2 is as follows: when applying $\hat{\Xi}^*$ in P-OPF-RS problem, the probability of constraint violation remains below ε with confidence $1 - \beta$:

$$\mathbb{P}^{N_s}\left[\mathcal{S} \in \mathcal{P}^{N_s} : \text{Vio}(\hat{\Xi}^*) \leq \varepsilon\right] \geq 1 - \beta,$$

with

$$\text{Vio}(\hat{\Xi}^*) := \mathbb{P}\left[\tilde{\boldsymbol{p}}^m \in \mathcal{P} : \hat{g}(\hat{\Xi}^*, \tilde{\boldsymbol{p}}^m) > 0\right] \ .$$

Remark 4: One can obtain an explicit expression for the desired number of scenarios N_s as in [32], where it is shown that given $\varepsilon, \beta \in (0, 1)$ then $N_s \geq \frac{e}{e-1}\frac{1}{\varepsilon}\left(d + \ln\frac{1}{\beta}\right)$.

Using the randomization technique explained above, we next provide an approximation technique to directly translate the infinite dimensional SDP of the C-OPF-RS problem into a finite dimensional SDP.

C. Infinite to Finite Program: Direct Approach

Rather than using the affine policy (12) proposed in (Section III-A) to obtain P-OPF-RS, and then, approximating $\mathcal{P}$ as in (Section III-B) to obtain SP-OPF-RS, one can also apply directly to the C-OPF-RS problem the randomization technique explained in (Section III-B) to formulate a finite-dimensional SDP. A slightly different idea has been

---

[3]These equality constraints cause numerical issues in the solver. Using a common practice in optimization (see, e.g., [29]), we implement these constraints by introducing a slack variable $u \in \mathbb{R}_+^2$ and rewriting each equality constraint $f(a) = b$ in the form of $b - u_1 \leq f(x) \leq b + u_2$. By adding L1-norm of slack variables as a penalty function into the objective function, u is minimized, essentially pushing $f(a)$ to be equal to b. It is important to highlight that using such a practical way to implement these equality constraints does not lead to any kind of relaxations, since they have been evaluated afterwords by checking the optimized value of the slack variables to confirm that they are sufficiently small.

TABLE I
WCCC ANALYSIS

SC-OPF-RS	$\mathcal{O}\left(T^{9.5}N_b^{6.5}N_G^{6.5}\log(1/\alpha)\right)$
SP-OPF-RS	$\mathcal{O}\left(T^6 N_b^4 N_G^4 \log(1/\alpha)\right)$

also considered in [8] using an ad-hoc manner. To this end, we recall $\mathcal{S} := \{\tilde{\boldsymbol{p}}^{m,1},\ldots,\tilde{\boldsymbol{p}}^{m,N_s}\} \in \mathcal{P}^{N_s}$ as a set of given finite scenarios and reformulate an approximated version of C-OPF-RS using the following optimization problem:

$$\text{SC-OPF-RS}: \begin{cases} \underset{\bar{\Xi}\in\mathcal{X}}{\text{minimize}} & f(\bar{\Xi}) \\ \text{subject to} & g(\bar{\Xi},\tilde{\boldsymbol{p}}^{m,i}) \leq 0 \,,\; \forall\tilde{\boldsymbol{p}}^{m,i}\in\mathcal{S} \end{cases},$$

where $\bar{\Xi}$ is the set of decision variables of SC-OPF-RS. It is important to note that $\bar{\Xi}$ is not the same set of optimizers (Ξ) of C-OPF-RS problem. The difference arises due to the equality constraints in (10) that lead to a new network state variable $\tilde{W}$ for each $\tilde{\boldsymbol{p}}^{m,i} \in \mathcal{S}$, and therefore,

$$\bar{\Xi} := \left\{\tilde{W}^f, \tilde{W}^1, \tilde{W}^2, \ldots, \tilde{W}^{N_s}, \tilde{\boldsymbol{d}}^{\text{us}}, \tilde{\boldsymbol{d}}^{\text{ds}}, \tilde{\boldsymbol{r}}^{\text{us}}, \tilde{\boldsymbol{r}}^{\text{ds}}\right\}.$$

The SC-OPF-RS problem is a finite-dimensional large-scale SDP, due to the fact that instead of a forecast and a generic network state, the set of decision variables now has extra N_s number of matrix variables (network states for all scenarios) in every time step, and each of the state matrices is also subject to PSD constraints. The minimum number of scenarios N_s to guarantee reasonable violation is typically quite large (see Remark 4). The resulting problem has therefore a high number of computationally expensive PSD constraints such that it is indeed computationally demanding.

To illustrate the advantages of SP-OPF-RS compared with SC-OPF-RS, we now analyze the WCCC for both problem formulations. If the resulting SDP is solved using an interior point method and a generic computational complexity of SDP formulation [33], [34] can be obtained via $\mathcal{O}\big((m^2n^2 + mn^3 + m^3)n^{1/2}\log(1/\alpha)\big)$ where n is the dimension of the decision variable and m is the number of constraints. In Table I, the problem dimensions and the resulting WCCCs are given, where N_s is assumed to be $\mathcal{O}(TN_G)$ for both formulations. It can be seen that the SP-OPF-RS problem has much lower order of WCCC. This increase in WCCC can be explained by the N_s repetitions of the state matrices.[4]

IV. DISTRIBUTED FRAMEWORK

A. Multi-Area Decomposition

We divide a power network into several control areas, and collect the indices in $\mathcal{A} := \{1,\ldots,N_a\}$. Define $\mathcal{N}_a \subset \mathcal{N}$ to be

the subset of buses corresponding to a control area $a \in \mathcal{A}$. Every bus belongs to exactly one control area, such that $\mathcal{N}_a \cap \mathcal{N}_b = \emptyset$ for all $a,b \in \mathcal{A}, a \neq b$, and $\bigcup_{a\in\mathcal{A}}\mathcal{N}_a = \mathcal{N}$. Consider now $\mathcal{B}_a$ as the set of neighboring control area indices that are connected to area a, such that for all $a \in \mathcal{A}$:

$$\mathcal{B}_a := \{b \in \mathcal{A} | \exists i \in \mathcal{N}_a, \exists j \in \mathcal{N}_b, (i,j) \in \mathcal{L},\}.$$

The lines that interconnect the areas are called tie-lines. These lines are collected into a tie-line set $\mathcal{T}_a \subset \mathcal{L}$ for all $a \in \mathcal{A}$:

$$\mathcal{T}_a := \{(i,j) \in \mathcal{L} | i \in \mathcal{N}_a, j \notin \mathcal{N}_a\}.$$

We now define the extended bus set $\mathcal{N}_a^+$ to expand the bus sets in each control area by including the endpoints of the tie-lines connected to that area for every $a \in \mathcal{A}$ as follows:

$$\mathcal{N}_a^+ := \mathcal{N}_a \cup \{j \in \mathcal{N} \mid \exists i \in \mathcal{N}_a, (i,j) \in \mathcal{T}_a\}.$$

We are now ready to decompose the matrix variable W into sub-matrices corresponding to the extended control areas. Consider $W_a \in \mathbb{S}^{2|\mathcal{N}_a^+|}$ as the network state of area a which is constructed by extracting a sub-matrix from W using only the rows and columns that correspond to the buses in $\mathcal{N}_a^+$. Denote the intersection of the extended bus sets by $\mathcal{E}_{ab} := \mathcal{N}_a^+ \cap \mathcal{N}_b^+$ for every neighboring area $b \in \mathcal{B}_a$. Consider now $[W_a]_{ab}$ as the sub-matrix extracted from W_a with its rows and columns corresponding to the buses in $\mathcal{E}_{ab}$, and likewise $[W_b]_{ab}$ the extraction from W_b that corresponds to the same buses. Note that the order of the subscript does not change the shared bus set between extended control areas, and therefore $[W_a]_{ab}$ and $[W_a]_{ba}$ refer to the same extraction from W_a.

Define the local feasibility set denoted with $\mathcal{W}_a(\boldsymbol{p}^w, \boldsymbol{s}^D)$ for all $a \in \mathcal{A}$ similar to (5) such that the power constraints are imposed for all $k \in \mathcal{N}_a$, the bus voltage constraints for all $k \in \mathcal{N}_a^+$, and the line flow limits for all $(l,m) \in (\mathcal{N}_a^+ \times \mathcal{N}_a^+) \cap \mathcal{L}$. The data-matrices, $Y_k, Y_k^*, Y_{lm}, Y_{lm}^*, M_k$, for each area $a \in \mathcal{A}$ are obtained via extracting the columns and rows corresponding to the buses in $\mathcal{N}_a^+$. These partitions of the data-matrices are denoted with $[\cdot]_a$ in $\mathcal{W}_a(\boldsymbol{p}^w, \boldsymbol{s}^D)$ for all $a \in \mathcal{A}$.

We now explain how one can decompose a PSD constraint. Consider a graph G over $\mathcal{N}$, with its edges corresponding to the set of extended buses $\{\mathcal{N}_a^+\}$ for all areas $a \in \mathcal{A}$. This means that every bus in $\mathcal{N}_a^+$ is connected to all other buses in $\mathcal{N}_a^+$ with a single edge to form a maximal clique. This graph is then chordal [17, Proposition 1] and all maximal cliques of G are captured by the subsets $\{\mathcal{N}_a^+\}$, under the following assumptions.

Assumption 2: Graph G with all control areas as its nodes and the tie-lines between the areas as its edges is a tree, i.e. an acyclic connected graph.

Assumption 3: Every control area $a \in \mathcal{A}$ has at least one bus that does not have overlap, i.e. does not have a tie-line connected to it.

Assumption 2 prevents multi-area power networks to have cyclic interconnections between their control areas. This can be achieved due to the fact that power networks are usually spread out geographically and mostly not intertwined. The typical number of tie-lines between power networks tends to be low. Assumption 3 will hold for almost every real-world power

---

[4]This concerns the WCCC for a problem with dense data-matrices, i.e. no assumption on the structure of the problem. Modern solvers, such as MOSEK [35], can achieve lower complexities by using sparsity in the problem structure. Whether or not this is the case for our problem, is outside the scope of this paper. For all IPM solvers, computational complexity scales logarithmically with $1/\alpha$, and polynomially with m and n, regardless of whether they make use of the problem structure or not.

system, as there tend to be much more buses than tie-lines in multi-area power networks.

The decomposition is valid if and only if these two assumptions hold, thus imposing PSD constraints on the sub-matrices corresponding to the extended areas, the original matrix will also be PSD, and can be completed from the local results. This enables one to split the single PSD constraint into $|\mathcal{A}|$ smaller PSD constraints.

B. Distributed Multi-Area SP-OPF-RS Problem Via ADMM

Our goal now is to decompose the SP-OPF-RS problem. Given Assumption 2 and Assumption 3, we approach this goal by imposing the following technical assumption.

Assumption 4: The set of scenarios of wind trajectories $\mathcal{S}$, as defined in Section III-B, is given to all control areas of the power network.

The condition in Assumption 4 is enforced due to the fact that the uncertainty source $\mathcal{P}$ is a common uncertainty source between all control areas, and therefore, the set of scenarios $\mathcal{S}$ has to be common between all control areas. We relax this condition later in this section.

Consider the following affine policy for the local network state of each area $\forall a \in \mathcal{A}$, $\forall \tilde{\boldsymbol{p}}^m \in \mathcal{S}$, and $\forall t \in \mathcal{T}$:

$$\hat{W}_{a,t}(\boldsymbol{p}_t^m) := W_{a,t}^f + \max(-\boldsymbol{p}_t^m, 0)W_{a,t}^{\text{us}} + \max(\boldsymbol{p}_t^m, 0)W_{a,t}^{\text{ds}},$$

where $W_{a,t}^f, W_{a,t}^{\text{us}}, W_{a,t}^{\text{ds}} \in \mathbb{S}^{2|\mathcal{N}_a^+|}$ are related to the sub-matrices from $W_t^f, W_t^{\text{us}}, W_t^{\text{ds}}$ using only the rows and columns corresponding to the buses in $\mathcal{N}_a^+$. Define the local reserve cost per each time step $t \in \mathcal{T}$ for all $a \in \mathcal{A}$ as follows:

$$f_R^a(\boldsymbol{r}_{a,t}^{\text{us}}, \boldsymbol{r}_{a,t}^{\text{ds}}) := \sum_{k \in \mathcal{G}_a} C_k^G \boldsymbol{c}^{\text{us}} C_k^G \boldsymbol{r}_{a,t}^{\text{us}} + \boldsymbol{c}^{\text{ds}} C_k^G \boldsymbol{r}_{a,t}^{\text{ds}},$$

where C_k^G is a connection matrix for the generators such that the (i, j)-th entry is one if generator j is located at the bus i and zero otherwise. Consider $\Xi_{\text{ma}} := \{\Xi_a\}_{\forall a \in \mathcal{A}}$ where $\Xi_a = \{\tilde{W}_a^f, \tilde{W}_a^{\text{us}}, \tilde{W}_a^{\text{ds}}, \tilde{\boldsymbol{r}}_a^{\text{us}}, \tilde{\boldsymbol{r}}_a^{\text{ds}}, \tilde{\boldsymbol{d}}_a^{\text{us}}, \tilde{\boldsymbol{d}}_a^{\text{ds}}\}$ is the set of local decision variables for each control area $a \in \mathcal{A}$, and define $\Theta := \{\tilde{W}_{ab}^f, \tilde{W}_{ab}^{\text{us}}, \tilde{W}_{ab}^{\text{ds}}, \tilde{\boldsymbol{d}}_a^{\text{us}}, \tilde{\boldsymbol{d}}_a^{\text{ds}}\}_{\forall b \in \mathcal{B}_a, \forall a \in \mathcal{A}}$ to be the set of auxiliary variables. We are now in the position to formulate a multi-area SP-OPF-RS problem (MASP-OPF-RS) as follows:

$$\min_{\Xi_{\text{ma}}, \Theta} \quad \sum_{a \in \mathcal{A}} \sum_{t \in \mathcal{T}} \left(f_G^a(W_{a,t}^f, \boldsymbol{p}_t^{w,f}) + f_R^a(\boldsymbol{r}_{a,t}^{\text{us}}, \boldsymbol{r}_{a,t}^{\text{ds}}) \right)$$

$$\text{s.t.} \quad W_{a,t}^f \in \mathcal{W}_a(\boldsymbol{p}_t^{w,f}, \boldsymbol{s}_t^D) \tag{15a}$$

$$\hat{W}_{a,t}(\boldsymbol{p}_t^m) \in \mathcal{W}_a(\boldsymbol{p}_t^{w,f} + \boldsymbol{p}_t^m, \boldsymbol{s}_t^D) \tag{15b}$$

$$W_{a,t}^f \succeq 0, \quad W_{a,t}^{\text{us}} \succeq 0, \quad W_{a,t}^{\text{ds}} \succeq 0 \tag{15c}$$

$$-\boldsymbol{r}_{a,t}^{\text{ds}} \leq \boldsymbol{r}_{a,t} \leq \boldsymbol{r}_{a,t}^{\text{us}}, \, 0 \leq \boldsymbol{r}_{a,t}^{\text{us}}, \, 0 \leq \boldsymbol{r}_{a,t}^{\text{ds}} \tag{15d}$$

$$\text{Tr}\left([Y_k]_a W_{a,t}^{\text{us}}\right) = C_k^G \boldsymbol{d}_{a,t}^{\text{us}}, \forall k \in \mathcal{G}_a \tag{15e}$$

$$\text{Tr}\left([Y_k]_a W_{a,t}^{\text{ds}}\right) = C_k^G \boldsymbol{d}_{a,t}^{\text{ds}}, \forall k \in \mathcal{G}_a \tag{15f}$$

$$\boldsymbol{1}^\top \boldsymbol{d}_{a,t}^{\text{us}} = 1, \, \boldsymbol{1}^\top \boldsymbol{d}_{a,t}^{\text{ds}} = -1 \tag{15g}$$

$$[W_{a,t}^f]_{ab} = \bar{W}_{ab,t}^f, \, \forall b \in \mathcal{B}_a \tag{15h}$$

$$[W_{a,t}^{\text{us}}]_{ab} = \bar{W}_{ab,t}^{\text{us}}, \, \forall b \in \mathcal{B}_a \tag{15i}$$

$$[W_{a,t}^{\text{ds}}]_{ab} = \bar{W}_{ab,t}^{\text{ds}}, \, \forall b \in \mathcal{B}_a \tag{15j}$$

$$\boldsymbol{d}_{a,t}^{\text{us}} = \bar{\boldsymbol{d}}_t^{\text{us}}, \, \boldsymbol{d}_{a,t}^{\text{ds}} = \bar{\boldsymbol{d}}_t^{\text{ds}} \tag{15k}$$

$$\forall \tilde{\boldsymbol{p}}^m \in \mathcal{S}, \, \forall t \in \mathcal{T}, \, \forall a \in \mathcal{A} \tag{15l}$$

where $\boldsymbol{r}_{a,t}$ should be replaced with

$$C_k^G \boldsymbol{r}_{a,t} = -\text{Tr}\left([Y_k]_a W_{a,t}^{\text{us}}\right) \min(\boldsymbol{p}_t^m, 0)$$
$$+ \text{Tr}\left([Y_k]_a W_{a,t}^{\text{ds}}\right) \max(\boldsymbol{p}_t^m, 0), \, \forall k \in \mathcal{G}_a.$$

The following proposition is a direct result of [36, Th. 1].

Proposition 2: The optimal objective function value of the MASP-OPF-RS problem is equal to the optimal objective function value of the SP-OPF-RS problem.

We now tackle the condition in Assumption 4 to provide a more flexible multi-area formulation of the MASP-OPF-RS problem. Define $\varepsilon_a \in (0, 1)$ and $\beta_a \in (0, 1)$ to be the local level of constraint violation and the local level of confidence for each control area $a \in \mathcal{A}$, respectively. Each control area can now build its own set of scenarios of wind power trajectories $\mathcal{S}_a := \{\tilde{\boldsymbol{p}}^{m,1}, \ldots, \tilde{\boldsymbol{p}}^{m,N_{s_a}}\}$ such that $N_{s_a} \geq \mathsf{N}(\varepsilon_a, \beta_a, d_a)$, where d_a is the number of decision variables in the control area $a \in \mathcal{A}$, as it is defined in Theorem 2. Using $\forall \tilde{\boldsymbol{p}}^m \in \mathcal{S}_a$ instead of $\forall \tilde{\boldsymbol{p}}^m \in \mathcal{S}$ in Equation (15l), we develop a more flexible multi-area formulation of the MASP-OPF-RS problem and relax Assumption 4. To quantify the robustness of the obtained solution via MASP-OPF-RS with $\mathcal{S}_a, \forall a \in \mathcal{A}$, consider the following theorem which is the main result of this section.

Theorem 3: Let $\varepsilon_a, \beta_a \in (0, 1), \forall a \in \mathcal{A}$ be chosen such that $\varepsilon = \sum_{a \in \mathcal{A}} \varepsilon_a \in (0, 1)$ and $\beta = \sum_{a \in \mathcal{A}} \beta_a \in (0, 1)$. If $\Xi_{\text{ma}}^* := \{\Xi_a^*\}_{\forall a \in \mathcal{A}}$ is a feasible solution of the MASP-OPF-RS problem with scenario set $\mathcal{S}_a$ for each $a \in \mathcal{A}$, then Ξ_{ma}^* is also a feasible solution of the P-OPF-RS problem with probability higher than $1 - \varepsilon$ and with confidence level of at least $1 - \beta$.

Proof: Based on an important observation that each control area $a \in \mathcal{A}$ can consider a common uncertainty source $\mathcal{S}$ as a local (private) source of uncertainty and build its own (local) set of scenarios $\mathcal{S}_a$, the proof follows the similar steps as [23, Theorem 2], that studies the quantification of the feasibility error with private and common uncertainty sources in a distributed setup using randomization technique, with some minor modifications. We provide a complete proof in the Appendix. ■

The following corollary is a direct result of Theorem 3. Decompose the P-OPF-RS problem using the proposed approach in Section IV-A into the multi-area P-OPF-RS problem (MAP-OPF-RS). This reformulation is straightforward and therefore it is omitted for the sake of brevity.

Corollary 1: The local optimal solution Ξ_a^* for all $a \in \mathcal{A}$ obtained via the MASP-OPF-RS problem is a feasible solution for the MAP-OPF-RS problem with probability higher than $1 - \varepsilon_a$ and with confidence level of $1 - \beta_a$.

We now continue by developing a distributed framework for the proposed formulation of the MASP-OPF-RS problem in (15). Define $\Lambda_{ab,t}^{f}, \Lambda_{ab,t}^{\mathrm{us}}, \Lambda_{ab}^{\mathrm{ds}} \in \mathbb{S}^{2|\mathcal{E}_{ab}|}$ for all $b \in \mathcal{B}_a$, for each $a \in \mathcal{A}$ at each time step $t \in \mathcal{T}$ as the multipliers for the first three consensus constraints, (15h), (15i), (15j), and $\lambda_{a,t}^{\mathrm{us}}, \lambda_{a,t}^{\mathrm{ds}} \in \mathbb{R}^{N_G}$ for all $a \in \mathcal{A}$ at each time step $t \in \mathcal{T}$ for the last two consensus constraints (15k). We then collect all the multipliers in Γ. One can denote the local objective function for each control area $a \in \mathcal{A}$ as:

$$f^a(\Xi_{\mathrm{a}}) := f_G^a\left(W_{a,t}^f, \boldsymbol{p}_t^{w,f}\right) + f_R^a\left(\boldsymbol{r}_{a,t}^{\mathrm{us}}, \boldsymbol{r}_{a,t}^{\mathrm{ds}}\right) + I_{W_a}(\Xi_{\mathrm{a}}),$$

where $I_{W_a}(\Xi_{\mathrm{a}})$ is a convex indicator function for all constraints except the consensus constraints. Consider now the augmented Lagrangian of the MASP-OPF-RS problem as follows:

$$
\begin{aligned}
L(\Xi_{\mathrm{ma}}, \Theta, \Gamma) = \sum_{a \in \mathcal{A}} \sum_{t \in \mathcal{T}} \Bigg\{ & f^a(\Xi_{\mathrm{a}}) \\
& + \frac{\mu}{2}\left\|\boldsymbol{d}_{a,t}^{\mathrm{us}} - \bar{\boldsymbol{d}}_t^{\mathrm{us}} + \frac{\lambda_{a,t}^{\mathrm{us}}}{\mu}\right\|_2^2 + \frac{\mu}{2}\left\|\boldsymbol{d}_{a,t}^{\mathrm{ds}} - \bar{\boldsymbol{d}}_t^{\mathrm{ds}} + \frac{\lambda_{a,t}^{\mathrm{ds}}}{\mu}\right\|_2^2 \\
& + \sum_{b \in \mathcal{B}_a} \left(\frac{\mu}{2}\left\|[W_{a,t}^f]_{ab} - \bar{W}_{ab,t}^f + \frac{\Lambda_{ab,t}^f}{\mu}\right\|_F^2 \right. \\
& \qquad + \frac{\mu}{2}\left\|[W_{a,t}^{\mathrm{us}}]_{ab} - \bar{W}_{ab,t}^{\mathrm{us}} + \frac{\Lambda_{ab,t}^{\mathrm{us}}}{\mu}\right\|_F^2 \\
& \qquad \left. + \frac{\mu}{2}\left\|[W_{a,t}^{\mathrm{ds}}]_{ab} - \bar{W}_{ab,t}^{\mathrm{ds}} + \frac{\Lambda_{ab,t}^{\mathrm{ds}}}{\mu}\right\|_F^2 + f(\Gamma) \right) \Bigg\},
\end{aligned}
$$

where $f(\Gamma)$ indicates terms that are related to the multipliers Γ. We now describe the steps of the ADMM algorithm as follows:

(1) Update Primal Variables: The multipliers and auxiliary variables are fixed at their value of the previous iteration. Consider the following minimization problem for all $a \in \mathcal{A}$:

$$
\begin{aligned}
\Xi_{\mathrm{a}}^{(k+1)} = \arg\min_{\Xi_{\mathrm{a}}} \sum_{t \in \mathcal{T}} \Bigg\{ & f^a(\Xi_{\mathrm{a}}) \\
& + \frac{\mu}{2}\left\|\boldsymbol{d}_{a,t}^{\mathrm{us}} - \bar{\boldsymbol{d}}_t^{\mathrm{us}} + \frac{\lambda_{a,t}^{\mathrm{us}}}{\mu}\right\|_2^2 + \frac{\mu}{2}\left\|\boldsymbol{d}_{a,t}^{\mathrm{ds}} - \bar{\boldsymbol{d}}_t^{\mathrm{ds}} + \frac{\lambda_{a,t}^{\mathrm{ds}}}{\mu}\right\|_2^2 \\
& + \sum_{b \in \mathcal{B}_a} \left(\frac{\mu}{2}\left\|[W_{a,t}^f]_{ab} - \bar{W}_{ab,t}^f + \frac{\Lambda_{ab,t}^f}{\mu}\right\|_F^2 \right. \\
& \qquad + \frac{\mu}{2}\left\|[W_{a,t}^{\mathrm{us}}]_{ab} - \bar{W}_{ab,t}^{\mathrm{us}} + \frac{\Lambda_{ab,t}^{\mathrm{us}}}{\mu}\right\|_F^2 \\
& \qquad \left. + \frac{\mu}{2}\left\|[W_{a,t}^{\mathrm{ds}}]_{ab} - \bar{W}_{ab,t}^{\mathrm{ds}} + \frac{\Lambda_{ab,t}^{\mathrm{ds}}}{\mu}\right\|_F^2 \right) \Bigg\}, \quad (16)
\end{aligned}
$$

where $f(\Gamma)$ is omitted, since the minimization is only in Ξ_{a}. This results in $|\mathcal{A}|$ number of small-scale SDPs in parallel, which can be considered the most computationally expensive step.

(2) Update Auxiliary Variables: The resulting $\Xi_{\mathrm{a}}^{(k+1)}$ for all $a \in \mathcal{A}$ are used to update the auxiliary variables. The multipliers again are fixed at their previous value. Note that each area only needs to communicate the part of its local variables

---

Algorithm 1: Distributed Stochastic MASP-OPF-RS.

1: Initialize: $k = 0, \Gamma^{(0)} = 0, \Theta^{(0)} = 0, \forall b \in \mathcal{B}_a$, $\forall a \in \mathcal{A}$
2: Fix $\varepsilon_a \in (0,1)$ and $\beta_a \in (0,1)$, $\forall a \in \mathcal{A}$ such that

$$\varepsilon = \sum_{a \in \mathcal{A}} \varepsilon_a \in (0,1), \ \beta = \sum_{a \in \mathcal{A}} \beta_a \in (0,1)$$

3: Build the set of local scenarios $\mathcal{S}_a$, $\forall a \in \mathcal{A}$
4: **while** not converged **do**
5:     **for all** $a \in \mathcal{A}$ **do**
6:         Update $\Xi_a^{(k+1)}$ using (16)
7:         Broadcast $[\Xi_a^{(k+1)}]_{ab}$ to all $b \in \mathcal{B}_a$
8:         Receive $[\Xi_a^{(k+1)}]_{ba}$ from all $b \in \mathcal{B}_a$
9:         Update $\Theta^{(k+1)}$ using (17) for all $b \in \mathcal{B}_a$
10:       Update $\Gamma^{(k+1)}$ using (18) for all $b \in \mathcal{B}_a$
11:       $k = k + 1$
12:     **end for**
13: **end while**

---

that have overlap with its neighboring area to update the auxiliary variables. If the multipliers are initialized with zero $\forall a \in \mathcal{A}, \forall b \in \mathcal{B}_a$, [37, Section 7.1], the update of the auxiliary variable simplifies to taking the average $\forall a \in \mathcal{A}, \forall b \in \mathcal{B}_a$:

$$
\begin{aligned}
\bar{W}_{ab,t}^{f,(k+1)} &= \frac{1}{2}\left([W_{a,t}^{f,(k+1)}]_{ab} + [W_{b,t}^{f,(k+1)}]_{ba}\right), \\
\bar{W}_{ab,t}^{\mathrm{us},(k+1)} &= \frac{1}{2}\left([W_{a,t}^{\mathrm{us},(k+1)}]_{ab} + [W_{b,t}^{\mathrm{us},(k+1)}]_{ba}\right), \\
\bar{W}_{ab,t}^{\mathrm{ds},(k+1)} &= \frac{1}{2}\left([W_{a,t}^{\mathrm{ds},(k+1)}]_{ab} + [W_{b,t}^{\mathrm{ds},(k+1)}]_{ba}\right), \\
\bar{\boldsymbol{d}}_t^{\mathrm{us},(k+1)} &= \frac{1}{|\mathcal{A}|}\sum_{a \in \mathcal{A}} \boldsymbol{d}_{a,t}^{\mathrm{us},(k+1)}, \\
\bar{\boldsymbol{d}}_t^{\mathrm{ds},(k+1)} &= \frac{1}{|\mathcal{A}|}\sum_{a \in \mathcal{A}} \boldsymbol{d}_{a,t}^{\mathrm{ds},(k+1)} . \quad (17)
\end{aligned}
$$

(3) Update Multiplier Variables: The multipliers are updated as follows $\forall a \in \mathcal{A}, \forall b \in \mathcal{B}_a$:

$$
\begin{aligned}
\Lambda_{ab,t}^{f,(k+1)} &= \Lambda_{ab,t}^{f,(k)} + \mu\left([W_{a,t}^{f,(k+1)}]_{ab} - \bar{W}_{ab,t}^{f,(k+1)}\right), \\
\Lambda_{ab,t}^{\mathrm{us},(k+1)} &= \Lambda_{ab,t}^{\mathrm{us},(k)} + \mu\left([W_{a,t}^{\mathrm{us},(k+1)}]_{ab} - \bar{W}_{ab,t}^{f,(k+1)}\right), \\
\Lambda_{ab,t}^{\mathrm{ds},(k+1)} &= \Lambda_{ab,t}^{\mathrm{ds},(k)} + \mu\left([W_{a,t}^{\mathrm{ds},(k+1)}]_{ab} - \bar{W}_{ab,t}^{f,(k+1)}\right), \\
\lambda_{a,t}^{\mathrm{us},(k+1)} &= \lambda_{a,t}^{\mathrm{us},(k)} + \mu\left(\boldsymbol{d}_{a,t}^{\mathrm{us},(k+1)} - \bar{\boldsymbol{d}}_t^{\mathrm{us},(k+1)}\right), \\
\lambda_{a,t}^{\mathrm{ds},(k+1)} &= \lambda_{a,t}^{\mathrm{ds},(k)} + \mu\left(\boldsymbol{d}_{a,t}^{\mathrm{ds},(k+1)} - \bar{\boldsymbol{d}}_t^{\mathrm{us},(k+1)}\right) . \quad (18)
\end{aligned}
$$

Notice that no information exchange is needed for the update of the multiplier, since the parts of the state matrix of neighboring areas have already been communicated in the update of the auxiliary variables.

Algorithm 1 summarizes the proposed distributed stochastic framework using a consensus ADMM algorithm to solve the MASP-OPF-RS problem. Consider the energy sequence

$\left\{\xi^{(k)}\right\}_{k=1}^{+\infty}$ as a measure for convergence of Algorithm 1 as follows:

$$\xi^{(k)} = \sum_{a \in \mathcal{A}} \sum_{t \in \mathcal{T}} \left\{ \left\| \boldsymbol{d}_{a,t}^{\text{us}} - \bar{\boldsymbol{d}}_t^{\text{us}} \right\|_2^2 + \left\| \boldsymbol{d}_{a,t}^{\text{ds}} - \bar{\boldsymbol{d}}_t^{\text{ds}} \right\|_2^2 \right.$$

$$+ \sum_{b \in \mathcal{B}_a} \left(\| [W_{a,t}^{f,(k)}]_{ab} - \bar{W}_{ab,t}^{f,(k)} \|_F^2 \right.$$

$$+ \| [W_{a,t}^{\text{us},(k)}]_{ab} - \bar{W}_{ab,t}^{\text{us},(k)} \|_F^2$$

$$\left. \left. + \| [W_{a,t}^{\text{ds},(k)}]_{ab} - \bar{W}_{ab,t}^{\text{ds},(k)} \|_F^2 \right) \right\}. \tag{19}$$

If $\xi^{(k)}$ is sufficiently small, all control areas of the power network have reached consensus on Θ.

We assume that the Slaters constraint qualification [38] holds for the MASP-OPF-RS problem (15) meaning that the feasible set of the MASP-OPF-RS has a non-empty interior, and it thus admits at least one strictly feasible solution. We can now provide convergence of the proposed consensus ADMM in Algorithm 1.

Theorem 4: Assume that Slater's condition holds for the MASP-OPF-RS problem (15), and consider the iterative steps given in Algorithm 1. Then the following statements hold:

- The residual sequence $\{\xi^{(k)}\}$ tends to 0 in a non-increasing way as k goes to $+\infty$, and therefore, we have $\forall b \in \mathcal{B}_a$ and for each $a \in \mathcal{A}$ at each time step $t \in \mathcal{T}$:

$$[W_{a,t}^{f,(+\infty)}]_{ab} = [W_{b,t}^{f,(+\infty)}]_{ba} = \bar{W}_{ab}^{f,(+\infty)},$$

$$[W_{a,t}^{\text{us},(+\infty)}]_{ab} = [W_{b,t}^{\text{us},(+\infty)}]_{ba} = \bar{W}_{ab}^{\text{us},(+\infty)},$$

$$[W_{a,t}^{\text{ds},(+\infty)}]_{ab} = [W_{b,t}^{\text{ds},(+\infty)}]_{ba} = \bar{W}_{ab}^{\text{ds},(+\infty)},$$

and $\forall a \in \mathcal{A}$ at each time step $t \in \mathcal{T}$:

$$\boldsymbol{d}_{a,t}^{\text{us},+\infty} = \bar{\boldsymbol{d}}_t^{\text{us},+\infty}, \; \boldsymbol{d}_{a,t}^{\text{ds},+\infty} = \bar{\boldsymbol{d}}_t^{\text{ds},+\infty}.$$

- The sequence $\{\Xi_a^{(k)}\}_{\forall a \in \mathcal{A}}$ converges to an optimal solution $\{\Xi_a^*\}_{\forall a \in \mathcal{A}}$ of the MASP-OPF-RS problem (15) as k tends to $+\infty$.

Proof: The theorem follows from [39] that studies the convergence of a standard ADMM problem. The details are omitted for brevity. ∎

V. NUMERICAL STUDY

In this section, we carry out numerical simulation studies to illustrate the performance of the proposed formulations and distributed framework. After a short description of the simulation setup, we present the simulation results in two different parts. We first provide a simulation study for the IEEE 30-bus power system using the proposed formulation in the SP-OPF-RS problem and compare it with the stochastic RS problem using a DC model of power network. We also develop a new benchmark formulation, namely a converted DC (CDC) approach to have a more sophisticated comparison [40]. As the second part of simulation results, we construct a realistic multi-area case study, and then, solve the MASP-OPF-RS problem using the

proposed distributed consensus framework in Section IV. We also provide a comparison using the SP-OPF-RS problem. It is important to highlight that the main reason why we focused on a two-area control power system is due to the fact that the proposed centralized formulation, SP-OPF-RS, is computationally demanding for larger networks (more than 30 buses is not computationally feasible). Therefore, to allow a complete detailed comparison, we focused on a 28-bus power network for the centralized version and two areas each consisting of 14 buses for the distributed framework.

A. Simulation Setup

We fix $\varepsilon = 10^{-2}$ and $\beta = 10^{-5}$ to obtain the number of required scenarios of wind power trajectories at each hour $N_s = 541$ as in Remark 4. To generate trajectories for the wind power, we follow the approach of [41] together with a data-set corresponding to the hourly aggregated wind power production of Germany over the period 2006-2011. The nominal load power is obtained from MATPOWER and multiplied with a time-varying load profile similar to [40]. We perform Monte Carlo simulations to check the violation probability of the solutions a posteriori for both parts of simulation results. Power flows of the network are simulated for 10000 new wind power trajectories using MATPOWER, where the power and voltage magnitude of generators and all the loads are fixed without imposing any constraints. The wind power is implemented as a negative load on the wind-bus. Afterward, the resulting power flows and voltage magnitudes are evaluated by means of counting the number of violated constraints. To solve all proposed formulations, we use Matlab together with YALMIP [42] as an interface and MOSEK [35] as a solver. All optimizations are run on a MacBook Pro with a 2, 4 GHz Intel Core i5 processor and 8 GB of RAM.

B. Simulation Results: Part One

We carried out a simulation study using the 30-bus IEEE benchmark power system [43], where only a single wind-bus infeed at bus 10 is considered.

After obtaining a solution, the scheduled generator power (the generator power based on the forecast wind trajectory) and the voltage magnitudes are extracted from $\tilde{W}^f = \{W_t^f\}_{t \in \mathcal{T}}$ for all time steps using the following relations $\forall k \in \mathcal{G}, \forall t \in \mathcal{T}$:

$$p_{k,t}^G = \text{Tr}\left(Y_k W_t^f\right) + p_{k,t}^D - p_{k,t}^w, \tag{20a}$$

$$q_{k,t}^G = \text{Tr}\left(Y_k^* W_t^f\right) + q_{k,t}^D, \tag{20b}$$

$$|v_{k,t}| = \sqrt{W_t^f(k,k) + W_t^f(N_b + k, N_b + k)}. \tag{20c}$$

A DC model of the power network is used to solve the OPF-RS problem as a benchmark approach for comparison purposes. A detailed description of the DC model can be obtained from [3] and [4]. The solution of the benchmark program is the real generator power and distribution vectors for every hour, $\left\{ \boldsymbol{p}_t^{G,\text{dc}}, \boldsymbol{d}_t^{\text{us,dc}}, \boldsymbol{d}_t^{\text{ds,dc}} \right\}$. One also needs the reactive generator power and generator voltage magnitudes in order to have a more
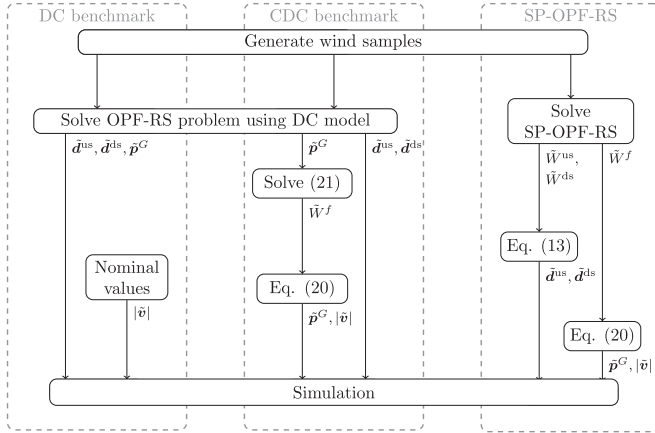
Fig. 1. Schematic overview of optimization and simulation process for the DC, CDC benchmarks, and the SP-OPF-RS.
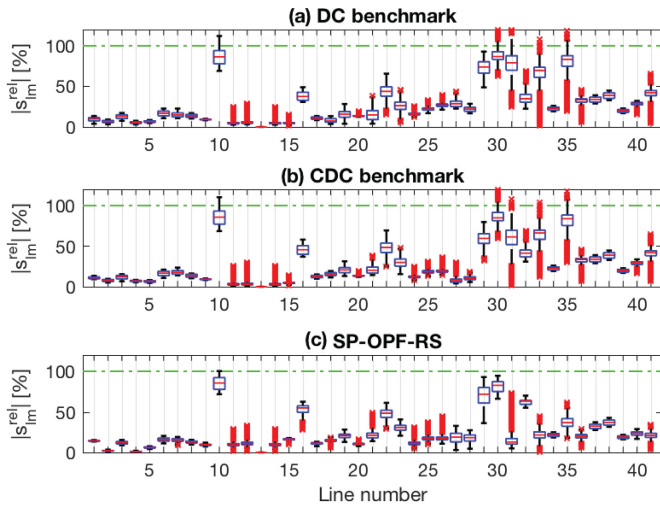

Fig. 2. Relative line loading for all hours and scenarios per line for the IEEE 30-bus benchmark case study. The red line represents the median value, edges of each box correspond to the 25th and 75th percentiles, the whiskers extend to 99% coverage, and the red marks denote the data outliers. The upper plots (a) and (b) show the Benchmark results, and the lower plot (c) shows the SP-OPF-RS solutions.

realistic comparison. In [8], the nominal value of such variables were extracted from the MATPOWER test case for all time steps and scenarios. This is called the nominal DC solution. This will result in large violations, since the reactive generator power is not adapted to the time-varying demand.

We here develop a novel benchmark approach, namely converted DC (CDC), to have a more sophisticated comparison by solving the following program:

$$
\min_{\tilde{W}} \quad \sum_{t \in \mathcal{T}} \sum_{k \in \mathcal{G}} \left(p_{k,t}^{G,\mathrm{dc}} - \left(\mathrm{Tr}\left(Y_k W_t \right) + p_{k,t}^{D} - p_{k,t}^{w,f} \right) \right)^2
$$

$$
\text{s.t.} \quad W_t \in \mathcal{W}(\boldsymbol{p}_t^{w,f}, \boldsymbol{s}_t^{D}), \qquad \forall t \in \mathcal{T},
$$

$$
W_t \succeq 0 \qquad \forall t \in \mathcal{T}. \tag{21}
$$

The solution to this program is a feasible (AC) network state $\tilde{W} = \{W_t\}_{t \in \mathcal{T}}$ where the real generator power is as close as possible to the obtained real generator power from the DC solu-
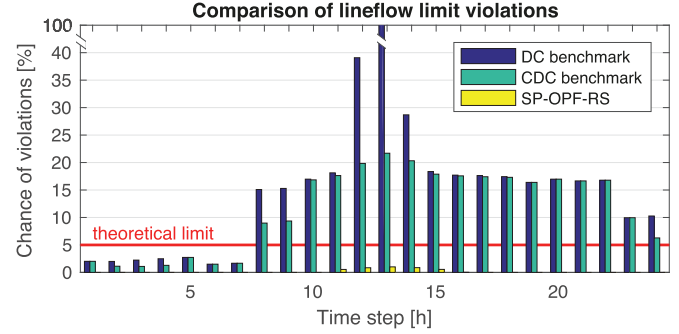

Fig. 3. Empirical violation level of lineflow limit for different formulations for the IEEE 30-bus benchmark case study.
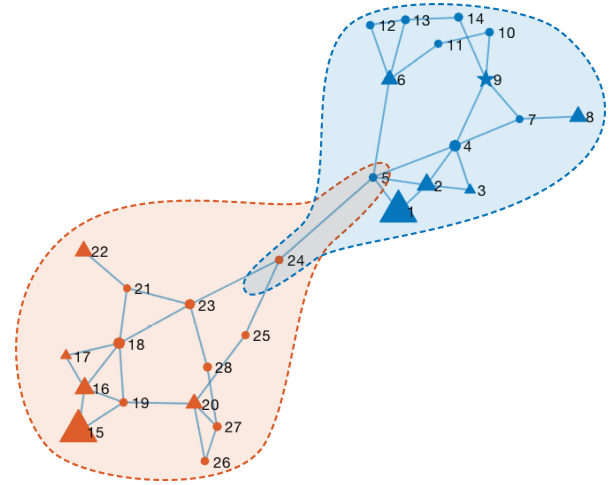

Fig. 4. Pictorial overview of the decomposed IEEE 28-bus power system case study. Triangles, circles, and a star indicate the generator buses, load buses and the wind bus, respectively. The size of each symbol indicates the respective generator capacity or load power. The different colors of the buses indicate the different control areas of the power network, and the shaded areas depict the extended control areas.
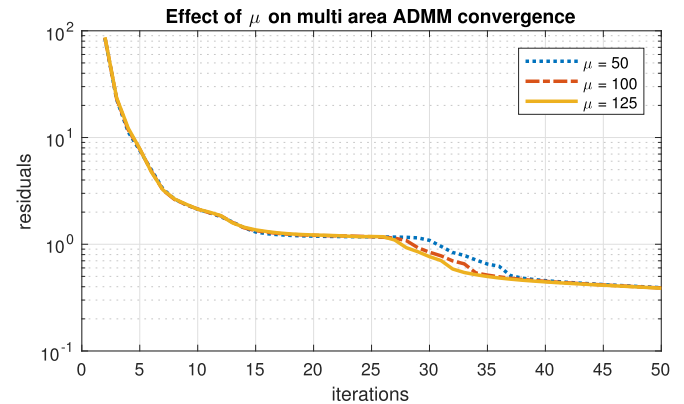

Fig. 5. Effect of varying μ on the convergence of ADMM.

tion. The distribution vectors used in simulation will be equal to those obtained from the original solution of the DC framework. A schematic overview of the optimization and simulation process to obtain and validate both the benchmark and proposed formulations is given in Fig. 1.
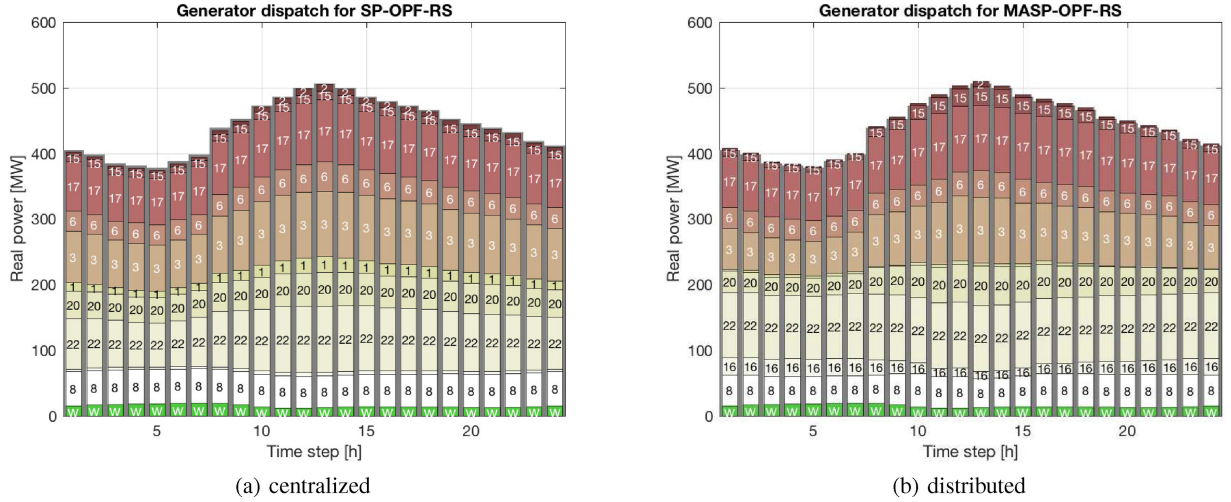
Fig. 6. Generator dispatch per hour for centralized and distributed solutions for the 28-bus test case. The grey shaded area corresponds to the total demand per hour. The numbers correspond to the generator buses, and the lowest part of each bar (green) indicates the wind power per hour.

The relative line loadings for all hours and scenarios are shown as box plots per line in Fig. 2 for DC, CDC, and SP-OPF-RS solutions. The relative line loading is defined as the apparent power flow over a line divided by the line rating $\forall (l,m) \in \mathcal{L}$:

$$|s_{lm}^{\text{rel}}| := \frac{|s_{lm}|}{|\overline{s}_{lm}|},$$

such that a loading higher than 100% corresponds to a violation of the lineflow limit. The DC benchmark results (Fig. 2a) shows the biggest violations, followed by the CDC benchmark results (Fig. 2b). For both benchmark results, line 10, 30, 31, and 35 are violated since the line loadings are overloaded as it is clearly shown in Fig. 2a-b. The SP-OPF-RS solutions (Fig. 2c) shows almost no violations for all hours and scenarios.

To further assess the performance of these results, the number of violating[5] network states is counted for each hour, and divided by the total number of scenarios to be an empirical measure of the probability on constraint violation per hour (see Fig. 3). As expected, the DC solution shows a very high level of violation during the peak hours, $t \geq 8$. Although the CDC solution improves the chance of lineflow limit violation, the theoretical limit at the peak hours is still not respected. It is important to notice that the empirical chance of constraint violation for the SP-OPF-RS results are much below the theoretical limit (5%) with 0.05% at $t = 13$ being the highest empirical probability.

We next examine the bus voltage magnitudes. It is observed that the DC, and the SP-OPF-RS solutions are always within the limits for all hours and scenarios. However, for the CDC formulation the bus voltage limits show a violation of 100% for all hours. This can be explained by the fact that in the DC framework, the bus voltages are assumed to be constant at nominal value. When we implement the obtained solution in the AC framework, it can be seen that this assumption does not hold. We can thus conclude that for both the DC formulations, the empirical chance of constraint violation is much above the theoretical limits once the solution is implemented in the AC

power flow simulations. The a-priori probabilistic guarantees are deemed valid for the SP-OPF-RS solutions.

C. Simulation Results: Part Two

We construct a two-area power network using two identical IEEE 14-bus power networks [43], and then connect a tie-line between bus 5 of the first network and bus 10 of the second network to create a realistic case study, resulting in an overall 28-bus power network with two control areas. The extended control areas are obtained by adding the endpoints of the tie-lines to the areas such that the buses are grouped in two overlapping sets as shown in Fig. 4. We formulate the MASP-OPF-RS problem (15) and then use Algorithm 1 to solve the problem in a distributed consensus framework using ADMM algorithm and coordinate the local solutions of the control areas towards convergence. Algorithm 1 is run until the residual sequence $\xi^{(k)}$ is sufficiently small, i.e. below 10^{-2} for each hour, and then, the solutions of current iterates (k) are used as the optimal solutions. This happens after 158 iterations. The step size μ is selected using a heuristic approach and it is fixed to 100 which results in good performance, while convergence is fast enough (see Fig. 5). We also formulate the SP-OPF-RS problem for the 28-bus power network and solve it in a centralized fashion for comparison purposes.

The resulting dispatch and distribution vectors are extracted from the final iterates. The generator dispatch is compared with the centralized solution in Fig. 6. The distributed solution is almost the same as the centralized solution. The distribution vectors are displayed in Fig. 7. It can be seen that the results are quite similar for the centralized and distributed results. The upspinning reserve is completely provided by the generator with the lowest cost which is generator number 8. The downspinning reserve is distributed over the first and second generator for the distributed solution, but in the centralized approach it is mostly provided by generator 8. For both the centralized and distributed solutions, the reserve is distributed over more generators during

---

[5] A network state is violating if at least one of the line limits is not satisfied.
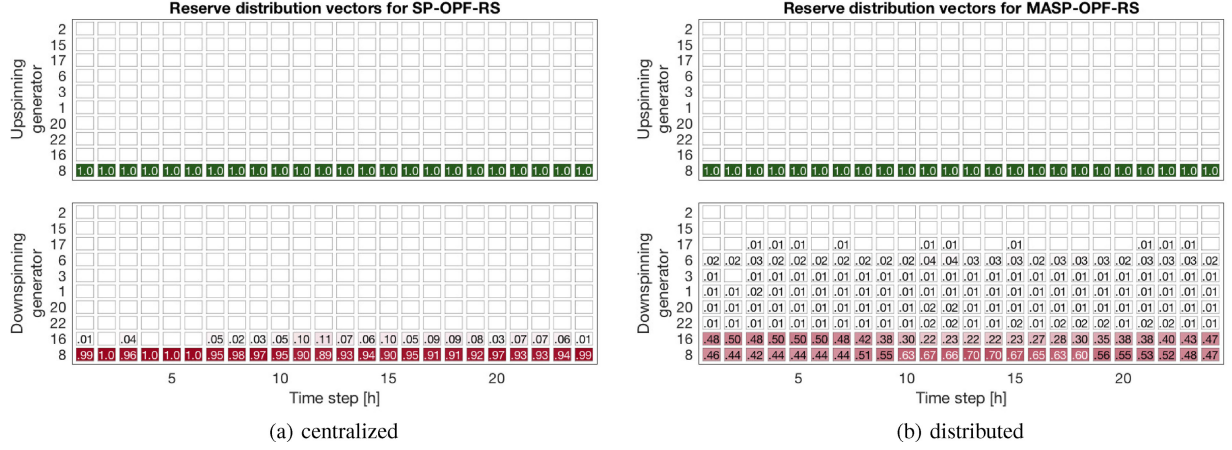
Fig. 7. Graphical display of up- and downspinning reserve distribution vectors per generator and hour for centralized and distributed solutions for the 28-bus test case. Darker cells correspond to higher contribution to the reserve power.
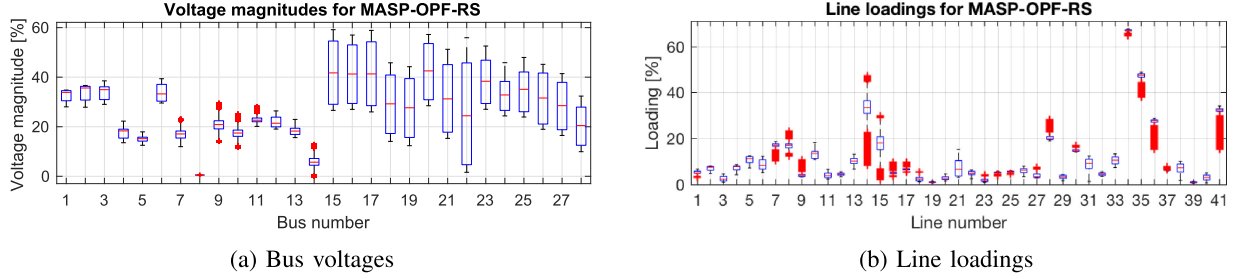

Fig. 8. Relative bus voltages and line loading for all hours and scenarios per line for the 28-bus test case. The red line represents the median value, edges of each box correspond to the 25th and 75th percentiles, the whiskers extend to 99% coverage, and the red marks denote the data outliers.

the peak hours, because the dispatch of the generators is higher in those hours, so less reserve power is available per generator.

We next simulate the resulting solutions with a new set of 10000 wind trajectories to compare the violation levels. The relative voltage magnitudes per bus, defined as $\forall k \in \mathcal{N}$:

$$|v_k^{\mathrm{rel}}| := \frac{|v_k| - |\underline{v_k}|}{|\overline{v_k}| - |\underline{v_k}|},$$

such that a relative voltage magnitude below 0% corresponds to a bus voltage which is below the lower limit, and a relative voltage magnitude greater than 100% indicates a violation of the upper limit. There is no violation of the voltage magnitude limits for any of the results for all time steps and scenarios as shown in Fig. 8a as predicted by our analysis of the developed methods. The relative line loadings for all hours and trajectories are shown as box plots per line in Fig. 8b. The number of violating network states divided by the total number of simulations returns an empirical measure of the violation probability. Both the centralized and distributed solutions have a very low violations probability: at most 0.02% and 0.06% at the peak hours, respectively. We can therefore conclude that the probabilistic guarantees are valid for the distributed solution.

VI. CONCLUSION

We developed a framework to carry out a multi-area RS using an AC OPF model with wind power generation by distributed

consensus using ADMM. The OPF-RS problem is formulated as a large-scale SDP in infinite-dimensional spaces, and then a novel affine policy is proposed to provide an approximation for the infinite-dimensional SDP by a finite-dimensional SDP together with explicitly quantified performance of the approximation. The proposed methodology bridges the gap between the DC and AC OPF model of power systems for RS and furnishes the TSOs with a tuning knob associated with the level of affordable probabilistic security.

Using the geographical pattern of the power system, a technique to decompose the large-scale system into a multi-area power network is provided. The consensus ADMM algorithm is then proposed to find a feasible solution for both local and overall multi-area network such that at every iteration, each area of power network solves a small-scale SDP problem, and then communicates some information to its neighbors to achieve consensus. By deriving a Lyapunov-type non-increasing function, it is shown that the proposed algorithm converges as long as Slater's condition holds. Using our distributed stochastic framework, each area can have its own wind information to achieve local feasibility certificates, while preserving overall feasibility of the multi-area power network under mild conditions.

Our theoretical developments have been demonstrated in simulation studies using IEEE benchmark power systems. The violation levels for the decomposed and centralized solutions are checked using power flow simulations to validate our

decomposition method which allows for distributed solving of OPF-RS type problems.

Our current work concentrates on the following main direction. We aim to extend our results to the case where the unit commitment (UC) formulation is added to the problem, similar to [22, Ch. 3] and the recent work in [44]. The authors in [44] proposed an approach to efficiently address OPF-UC problem based on sparsity-exploiting techniques (Lasserre relaxations [45]). This can be an immediate extension to our proposed formulation and distributed framework.

APPENDIX

Proof of Theorem 1: P-OPF-RS problem is an inner approximation version of C-OPF-RS problem [46, Definition 12.2.13], which is exact if we show that the gap between their objective function values is zero. This can be shown using the fact that the difference between optimizers Ξ^* of C-OPF-RS and the projection of Ξ^* onto the feasible set of P-OPF-RS is zero, since C-OPF-RS and P-OPF-RS have clearly similar objective functions.

In order to show the difference between the optimizers Ξ^* and the optimizer $\hat{\Xi}^*$ (the projection of Ξ^* onto the feasible set of P-OPF-RS), we need to establish equivalence between constraints of both problems using the proposed policy in (12). It is important to notice that the proposed affine policy (12) is obtained by algebraic manipulation of the reserve power definition in (10).

By comparing C-OPF-RS and P-OPF-RS, it is clear that the first and second constraints in P-OPF-RS are the same as (7b) and (7c), respectively, where W_t is replaced by $\hat{W}_t(\boldsymbol{p}_t^m)$, following the proposed affine policy in (12). As for the constraint (7d), we use the following equivalent constraints using a conic combination concept[6] of matrix variables, called coefficient matrices:

$$\hat{W}_t(\boldsymbol{p}_t^m) \succeq 0 \quad \longleftrightarrow \quad W_t^f \succeq 0, W_t^{\text{us}} \succeq 0, W_t^{\text{ds}} \succeq 0 .$$

Imposing PSD constraints on the coefficient matrices is equivalent to imposing a PSD constraint on the proposed policy for the network state in (12), since $\max(\boldsymbol{p}_t^m, 0) \geq 0$, $\max(-\boldsymbol{p}_t^m, 0) \geq 0$, $\forall \boldsymbol{p}_t^m \in \mathcal{P}$, together with the fact that any conic combination of PSD matrices is a PSD matrix [25, Section 2.2.5], thus the approximated network state $\hat{W}_t(\boldsymbol{p}_t^m)$ is guaranteed to be PSD.

We now examine the definition of reserve power expressed with the new parametrization $\hat{W}_t(\boldsymbol{p}_t^m)$:

$$r_{k,t} = p_{k,t}^G - p_{k,t}^{G,f} = \text{Tr}\left(Y_k\left(\hat{W}(\boldsymbol{p}_t^m) - W_t^f\right)\right)$$

$$= \text{Tr}\left(Y_k\left(\max(-\boldsymbol{p}_t^m, 0)W_t^{\text{us}} + \max(\boldsymbol{p}_t^m, 0)W_t^{\text{ds}}\right)\right)$$

$$= -\text{Tr}\left(Y_k W_t^{\text{us}}\right)\min(\boldsymbol{p}_t^m, 0) + \text{Tr}\left(Y_k W_t^{\text{ds}}\right)\max(\boldsymbol{p}_t^m, 0),$$

where the last equation is similar to the above assertion by using the linearity of the trace operator and the fact that $\forall \alpha \in \mathbb{R}, \max(-\alpha, 0) = -\min(\alpha, 0)$.

The last two constraints are similar to the constraints (11) to ensure that the reserve powers will always be the exact opposite

[6]A *conic combination* is a linear combination with only non-negative coefficients, see also [25, Section 2.1.5].

of the mismatch power. By summing the previous result over all generators $k \in \mathcal{G}$:

$$\sum_{k \in \mathcal{G}} r_{k,t} = -\overbrace{\sum_{k \in \mathcal{G}} \text{Tr}\left(Y_k W_t^{\text{us}}\right)}^{=1} \min(\boldsymbol{p}_t^m, 0)$$

$$+ \overbrace{\sum_{k \in \mathcal{G}} \text{Tr}\left(Y_k W_t^{\text{ds}}\right)}^{=-1} \max(\boldsymbol{p}_t^m, 0),$$

$$= -\min(\boldsymbol{p}_t^m, 0) - \max(\boldsymbol{p}_t^m, 0) = -\boldsymbol{p}_t^m .$$

The proof is completed by noting that $\tilde{W}^{\text{us}}$ and $\tilde{W}^{\text{ds}}$ are related to changes in the network state by the distribution of up- and downspinning reserve power, respectively. Moreover, the proposed equality constraints are feasible due to fact that Y_k is indefinite for all $k \in \mathcal{G}$.   ∎

Proof of Theorem 3: Consider $\hat{\Xi}^*$ to be the optimizer of the SP-OPF-RS problem and define $\text{Vio}(\hat{\Xi}^*)$ to be the violation probability of the P-OPF-RS constraints as follows:

$$\text{Vio}(\hat{\Xi}^*) := \mathbb{P}\left[\tilde{\boldsymbol{p}}^m \in \mathcal{P} : \hat{\Xi}^* \notin \tilde{\mathcal{X}}(\tilde{\boldsymbol{p}}^m)\right], \quad (22a)$$

where $\tilde{\mathcal{X}}(\tilde{\boldsymbol{p}}^m)$ is the uncertain feasible region of the P-OPF-RS problem, and it can be characterized via its constraints. Following Theorem 2, we have

$$\mathbb{P}^{N_s}\left[\mathcal{S} \in \mathcal{P}^{N_s} : \text{Vio}(\hat{\Xi}^*) \leq \varepsilon\right] \geq 1 - \beta . \quad (22b)$$

Given Assumption 2 and Assumption 3 together with Proposition 2, the MASP-OPF-RS problem is an exact decomposition of the SP-OPF-RS problem. This yields the following equivalence relations:

$$\begin{cases} \hat{\Xi}^* := \Xi_{\text{ma}}^* = \{\Xi_a^*\}_{\forall a \in \mathcal{A}} \\ \tilde{\mathcal{X}}(\tilde{\boldsymbol{p}}^m) := \prod_{a \in \mathcal{A}} \tilde{\mathcal{X}}_a(\tilde{\boldsymbol{p}}^m) \end{cases}, \quad (23)$$

where $\Xi_{\text{ma}}^* = \{\Xi_a^*\}_{\forall a \in \mathcal{A}}$ is the set of optimizers of the MASP-OPF-RS problem with Ξ_a^* as the optimizer of each control area $a \in \mathcal{A}$. Moreover, $\tilde{\mathcal{X}}_a(\tilde{\boldsymbol{p}}^m)$ represents the uncertain feasible set of each control area $a \in \mathcal{A}$ and it can be characterized using constraints of the MASP-OPF-RS problem for each control area $a \in \mathcal{A}$. To this end, it is necessary to prove that the above statements (22) are still hold under the aforementioned relations (23). We now break down the proof into two steps. We first show the results for each control area $a \in \mathcal{A}$, and then extend into a multi-area power system problem.

1) Define $\text{Vio}(\Xi_a^*)$ to be the violation probability of each control area $a \in \mathcal{A}$ for the P-OPF-RS problem as follows:

$$\text{Vio}(\Xi_a^*) := \mathbb{P}\left[\tilde{\boldsymbol{p}}^m \in \mathcal{P} : \Xi_a^* \notin \tilde{\mathcal{X}}_a(\tilde{\boldsymbol{p}}^m)\right] . \quad (24)$$

Applying the existing results in Theorem 2 for each control area $a \in \mathcal{A}$, we have

$$\mathbb{P}^{N_{s_a}}\left[\mathcal{S}_a \in \mathcal{P}^{N_{s_a}} : \text{Vio}(\Xi_a^*) \leq \varepsilon_a\right] \geq 1 - \beta_a . \quad (25)$$

2) Following the relations (23), it is easy to rewrite $\mathrm{Vio}(\hat{\Xi}^*)$ in the following form:

$$\mathrm{Vio}(\hat{\Xi}^*) = \mathrm{Vio}(\Xi_{\mathrm{ma}}^*) = \mathbb{P}\left[\tilde{\boldsymbol{p}}^m \in \mathcal{P} : \Xi_{\mathrm{ma}}^* \notin \prod_{a \in \mathcal{A}} \tilde{\mathcal{X}}_a(\tilde{\boldsymbol{p}}^m)\right],$$

It is then sufficient to show that for $N_s = \max_{a \in \mathcal{A}} N_{s_a}$:

$$\mathbb{P}^{N_s}\left[\mathcal{S} \in \mathcal{P}^{N_s} : \mathrm{Vio}(\Xi_{\mathrm{ma}}^*) \geq \varepsilon\right] \leq \beta, \qquad (26)$$

where $\varepsilon = \sum_{a \in \mathcal{A}} \varepsilon_a \in (0, 1)$ and $\beta = \sum_{a \in \mathcal{A}} \beta_a \in (0, 1)$. Hence

$$\mathrm{Vio}(\hat{\Xi}^*) = \mathrm{Vio}(\Xi_{\mathrm{ma}}^*) = \mathbb{P}\left[\tilde{\boldsymbol{p}}^m \in \mathcal{P} : \Xi_{\mathrm{ma}}^* \notin \prod_{a \in \mathcal{A}} \tilde{\mathcal{X}}_a(\tilde{\boldsymbol{p}}^m)\right]$$

$$= \mathbb{P}\left[\tilde{\boldsymbol{p}}^m \in \mathcal{P} : \exists a \in \mathcal{A}, \Xi_a^* \notin \tilde{\mathcal{X}}_a(\tilde{\boldsymbol{p}}^m)\right]$$

$$= \mathbb{P}\left[\bigcup_{a \in \mathcal{A}} \left\{\tilde{\boldsymbol{p}}^m \in \mathcal{P} : \Xi_a^* \notin \tilde{\mathcal{X}}_a(\tilde{\boldsymbol{p}}^m)\right\}\right]$$

$$\leq \sum_{a \in \mathcal{A}} \mathbb{P}\left[\tilde{\boldsymbol{p}}^m \in \mathcal{P} : \Xi_a^* \notin \tilde{\mathcal{X}}_a(\tilde{\boldsymbol{p}}^m)\right] = \sum_{a \in \mathcal{A}} \mathrm{Vio}(\Xi_a^*).$$

The last statement implies that $\mathrm{Vio}(\Xi_{\mathrm{ma}}^*) \leq \sum_{a \in \mathcal{A}} \mathrm{Vio}(\Xi_a^*)$, and thus, we have

$$\mathbb{P}^{N_s}\left[\mathcal{S} \in \mathcal{P}^{N_s} : \mathrm{Vio}(\Xi_{\mathrm{ma}}^*) \geq \varepsilon\right]$$

$$\leq \mathbb{P}^{N_s}\left[\mathcal{S} \in \mathcal{P}^{N_s} : \sum_{a \in \mathcal{A}} \mathrm{Vio}(\Xi_a^*) \geq \sum_{a \in \mathcal{A}} \varepsilon_a\right]$$

$$= \mathbb{P}^{N_s}\left[\bigcup_{a \in \mathcal{A}} \left\{\mathcal{S}_a \in \mathcal{P}^{N_{s_a}} : \mathrm{Vio}(\Xi_a^*) \geq \varepsilon_a\right\}\right]$$

$$\leq \sum_{a \in \mathcal{A}} \mathbb{P}^{N_{s_a}}\left[\mathcal{S}_a \in \mathcal{P}^{N_{s_a}} : \mathrm{Vio}(\Xi_a^*) \geq \varepsilon_a\right] \leq \sum_{a \in \mathcal{A}} \beta_a = \beta.$$

The obtained bounds in the above procedure are the desired assertions as it is stated in the theorem. The proof is completed by noting that the feasible set $\tilde{\mathcal{X}}(\tilde{\boldsymbol{p}}^m) = \prod_{a \in \mathcal{A}} \tilde{\mathcal{X}}_a(\tilde{\boldsymbol{p}}^m)$ of the MASP-OPF-RS has a non-empty interior, and it thus admits at least one feasible solution $\Xi_{\mathrm{ma}}^* = \{\Xi_a^*\}_{\forall a \in \mathcal{A}}$. ∎

REFERENCES

[1] A. Papavasiliou, S. Oren, and R. O'Neill, "Reserve requirements for wind power integration: A scenario-based stochastic programming framework," *IEEE Trans. Power Syst.*, vol. 26, no. 4, pp. 2197–2206, Nov. 2011.

[2] J. Warrington, P. J. Goulart, S. Mariéthoz, and M. Morari, "Robust reserve operation in power systems using affine policies," in *Proc. IEEE Conf. Decis. Control.*, 2012, pp. 1111–1117.

[3] K. Margellos, V. Rostampour, M. Vrakopoulou, M. Prandini, G. Andersson, and J. Lygeros, "Stochastic unit commitment and reserve scheduling: A tractable formulation with probabilistic certificates," in *Proc. IEEE Euro. Control Conf.*, 2013, pp. 2513–2518.

[4] M. Vrakopoulou, K. Margellos, J. Lygeros, and G. Andersson, "A probabilistic framework for reserve scheduling and N-1 security assessment of systems with high wind power penetration," *IEEE Trans. Power Syst.*, vol. 28, no. 4, pp. 3885–3896, Nov. 2013.

[5] G. Andersson, *Modelling and Analysis of Electric Power Systems*. Zurich, Switzerland: ETH Zürich Univ., 2008.

[6] B. Stott, J. Jardim, and O. Alsaç, "DC power flow revisited," *IEEE Trans. Power Syst.*, vol. 24, no. 3, pp. 1290–1300, Aug. 2009.

[7] J. Lavaei and S. H. Low, "Zero duality gap in optimal power flow problem," *IEEE Trans. Power Syst.*, vol. 27, no. 1, pp. 92–107, Feb. 2012.

[8] V. Rostampour, K. Margellos, M. Vrakopoulou, M. Prandini, G. Andersson, and J. Lygeros, "Reserve requirements in AC power systems with uncertain generation," in *Proc. IEEE Innovative Smart Grid Technol. Europe*, 2013, pp. 1–5.

[9] J. Dopazo, O. Klitin, and A. Sasson, "Stochastic load flows," *IEEE Trans. Power App. Syst.*, vol. PAS-94, pp. 299–309, Mar. 1975.

[10] W. Fu and J. D. McCalley, "Risk based optimal power flow," in *Proc. IEEE Porto Power Tech*, 2001, vol. 3, pp. 1–6.

[11] T. Wada, R. Morita, T. Asai, I. Masubuchi, and Y. Fujisaki, "A randomized algorithm for chance constrained optimal power flow with renewables," *J. Control, Meas., Syst. Integration*, vol. 10, no. 4, pp. 303–309, 2017.

[12] L. Roald and G. Andersson, "Chance-constrained AC optimal power flow: Reformulations and efficient algorithms," *IEEE Trans. Power Syst.*, vol. 33, no. 3, pp. 2906–2918, May 2018.

[13] M. Chamanbaz, F. Dabbene, and C. Lagoa, "AC optimal power flow in the presence of renewable sources and uncertain loads," unpublished paper, 2017. [Online]. Available: https://arxiv.org/abs/1702.02967v1

[14] A. Venzke, L. Halilbasic, U. Markovic, G. Hug, and S. Chatzivasileiadis, "Convex relaxations of chance constrained AC optimal power flow," *IEEE Trans. Power Syst.*, vol. 33, no 3, pp. 2829–2841, May 2018.

[15] R. A. Jabr, "Adjustable robust OPF with renewable energy sources," *IEEE Trans. Power Syst.*, vol. 28, no. 4, pp. 4742–4751, Nov. 2013.

[16] H. Ye, "Surrogate affine approximation based co-optimization of transactive flexibility, uncertainty, and energy," *IEEE Trans. Power Syst.*, vol. 33, pp. 4084–4096, Jul. 2018.

[17] H. Zhu and G. B. Giannakis, "Multi-area state estimation using distributed SDP for nonlinear power systems," in *Proc. IEEE Int. Conf. Smart Grid Commun.*, 2012, pp. 623–628.

[18] A. Y. Lam, B. Zhang, and N. T. David, "Distributed algorithms for optimal power flow problem," in *Proc. 51st IEEE Conf. Decis. Control*, 2012, pp. 430–437.

[19] D. K. Molzahn, J. T. Holzer, B. C. Lesieutre, and C. L. DeMarco, "Implementation of a large-scale optimal power flow solver based on semidefinite programming," *IEEE Trans. Power Syst.*, vol. 28, no. 4, pp. 3987–3998, Nov. 2013.

[20] R. Madani, A. Kalbat, and J. Lavaei, "ADMM for sparse semidefinite programming with applications to optimal power flow problem," in *Proc. 54th IEEE Conf. Decis. Control*, 2015, pp. 5932–5939.

[21] A. Kalbat and J. Lavaei, "A fast distributed algorithm for decomposable semidefinite programs," in *Proc. 54th IEEE Conf. Decis. Control*, 2015, pp. 1742–1749.

[22] V. Rostampour, "Tractable reserve scheduling formulations for power systems with uncertain generation," M.Sc. thesis, Politecnico di Milano, Milan, Italy, 2013.

[23] V. Rostampour and T. Keviczky, "Distributed stochastic model predictive control synthesis for large-scale uncertain linear systems," in *Proc. 2018 Annu. Amer. Control Conf.*, 2018, doi: 10.23919/ACC.2018.8431452

[24] J. M. Morales, A. J. Conejo, and J. Pérez-Ruiz, "Economic valuation of reserves in power systems with high penetration of wind power," *IEEE Trans. Power Syst.*, vol. 24, no. 2, pp. 900–910, May 2009.

[25] S. Boyd and L. Vandenberghe, *Convex Optimization*. Cambridge, U.K.: Cambridge Univ. Press, 2004.

[26] K. Lehmann, A. Grastien, and P. Van Hentenryck, "AC-feasibility on tree networks is NP-hard," *IEEE Trans. Power Syst.*, vol. 31, no. 1, pp. 798–801, Jan. 2016.

[27] Z.-Q. Luo, W.-K. Ma, A. M.-C. So, Y. Ye, and S. Zhang, "Semidefinite relaxation of quadratic optimization problems," *IEEE Signal Process. Mag.*, vol. 27, no. 3, pp. 20–34, May 2010.

[28] R. Madani, S. Sojoudi, and J. Lavaei, "Convex relaxation for optimal power flow problem: Mesh networks," *IEEE Trans. Power Syst.*, vol. 30, no. 1, pp. 199–211, Jan. 2015.

[29] A. Abur and M. K. Celik, "Least absolute value state estimation with equality and inequality constraints," *IEEE Trans. Power Syst.*, vol. 8, no. 2, pp. 680–686, May 1993.

[30] A. Ben-Tal, L. El Ghaoui, and A. Nemirovski, *Robust Optimization*. Princeton, NJ, USA: Princeton Univ. Press, 2009.

[31] M. C. Campi and S. Garatti, "The exact feasibility of randomized solutions of uncertain convex programs," *SIAM J. Optim.*, vol. 19, no. 3, pp. 1211–1230, 2008.

[32] T. Alamo, R. Tempo, A. Luque, and D. R. Ramirez, "Randomized methods for design of uncertain systems: Sample complexity and sequential algorithms," *Automatica*, vol. 52, pp. 160–172, 2015.

[33] R. D. C. Monteiro, "First- and second-order methods for semidefinite programming," *Math. Program.*, vol. 97, no. 1, pp. 209–244, 2003.

[34] S. Bubeck, "Convex optimization: Algorithms and complexity," *Found. Trends Mach. Learn.*, vol. 8, no. 3/4, pp. 231–357, 2015.

[35] E. Anderson, *The MOSEK Optimization Toolbox for MATLAB Manual*, (1999). [Online]. Available: http://docs.mosek.com/7.1/toolbox/index.html

[36] R. Madani, M. Ashraphijuo, and J. Lavaei, "Promises of conic relaxation for contingency-constrained optimal power flow problem," *IEEE Trans. Power Syst.*, vol. 31, no. 2, pp. 1297–1307, Mar. 2016.

[37] S. Boyd, "Distributed optimization and statistical learning via the alternating direction method of multipliers," *Found. Trends Mach. Learn.*, vol. 3, no. 1, pp. 1–122, 2010.

[38] M. Slater *et al.*, "Lagrange multipliers revisited," Cowles Foundation for Research in Economics, Yale University, Tech. Rep., 1959.

[39] B. He and X. Yuan, "On non-ergodic convergence rate of Douglas–Rachford alternating direction method of multipliers," *Numerische Mathematik*, vol. 130, no. 3, pp. 567–577, 2015.

[40] V. Rostampour, O. ter Haar, and T. Keviczky, "Tractable reserve scheduling in AC power systems with uncertain wind power generation," in *Proc. IEEE 56th Annu. Conf. Decis. Control*, 2017, pp. 2647–2654.

[41] G. Papaefthymiou and B. Klockl, "MCMC for wind power simulation," *IEEE Trans. Energy Convers.*, vol. 23, no. 1, pp. 234–240, Mar. 2008.

[42] J. Löfberg, "Yalmip: A toolbox for modeling and optimization in MATLAB," in *Proc. IEEE Int. Symp. Comput. Aided Control Syst. Des.*, 2004, pp. 284–289.

[43] R. Christie, "Power systems test case archive," University of Washington, Seattle, WA, USA, 2000. [Online]. Available: http://www2.ee.washington.edu/research/pstca

[44] E. Dumon, M. Ruiz, H. Godard, and J. Maeght, "SDP resolution techniques for the optimal power flow with unit commitment," in *Proc. IEEE Manchester PowerTech.*, 2017, pp. 1–6.

[45] J. B. Lasserre, "Global optimization with polynomials and the problem of moments," *SIAM J. Optim.*, vol. 11, no. 3, pp. 796–817, 2001.

[46] O. Hernández-Lerma and J. B. Lasserre, *Further Topics on Discrete-Time Markov Control Processes*, vol. 42. New York, NY, USA: Springer-Verlag, 2012.

Ole ter Haar received the B.Sc. degree in mechanical engineering and the M.Sc. degree in control engineering (cum laude) from the Delft University of Technology, Delft, the Netherlands, in 2015 and 2017, respectively.

During his masters, he was an intern for a semester with General Electric Global Research, Munich, Germany to develop a computer vision algorithm for automated inspection. He is currently an Associate with the Boston Consulting Group, Boston, MA, USA. His research interests include optimization, machine learning, and modeling.

Tamás Keviczky received the M.Sc. degree in electrical engineering from the Budapest University of Technology and Economics, Budapest, Hungary, in 2001, and the Ph.D. degree from the Control Science and Dynamical Systems Center, University of Minnesota, Minneapolis, MN, USA, in 2005.

He is currently an Associate Professor with the Delft Center for Systems and Control, Delft University of Technology, Delft, the Netherlands. He was a Postdoctoral Scholar in control and dynamical systems with the California Institute of Technology, Pasadena, CA, USA. His research interests include distributed optimization and optimal control, model predictive control, embedded optimization-based control, and estimation of large-scale systems with applications in aerospace, automotive, mobile robotics, industrial processes, and infrastructure systems, such as water, heat, and power networks.

Dr. Keviczky was a corecipient of the AACC O. Hugo Schuck Best Paper Award for Practice in 2005. He was an Associate Editor for *Automatica* between 2011 and 2017.

Vahab Rostampour received the M.Sc. degree in automation and control engineering from the Politecnico di Milano, Milan, Italy, in 2013, and the Ph.D. degree from the Delft Center for Systems and Control, Delft University of Technology, Delft, the Netherlands, in 2018.

He is currently a Postdoctoral Researcher with the Engineering and Technology Institute, University of Groningen, Groningen, the Netherlands. His research interests include control synthesis and analysis, distributed learning and optimization of dynamical systems, and decision making in uncertain dynamical environments, with applications to large-scale systems such as thermal grids and power networks.